REPORT DOCUMENTATION PAGE

Form Approved
OMB NO. 0704-0188

1. AGENCY USE ONLY (Leave Blank)	2. REPORT DATE	3. REPORT TYPE AND DATES COVERED
	1/15/05	Final Report 9/25/00 - 9/24/04

4. TITLE AND SUBTITLE
New Catalysts for the Destruction of Chemical Warfare Agents

5. FUNDING NUMBERS
DAAD 19-00-1-0557

6. AUTHOR(S)
Donna A. Chen

7. PERFORMING ORGANIZATION NAME(S) AND ADDRESS(ES)
University of South Carolina
Department of Chemistry and Biochemistry
631 Sumter Street, Columbia, SC 29208

8. PERFORMING ORGANIZATION REPORT NUMBER
13020-FA00

9. SPONSORING / MONITORING AGENCY NAME(S) AND ADDRESS(ES)
U. S. Army Research Office
P.O. Box 12211
Research Triangle Park, NC 27709-2211

10. SPONSORING / MONITORING AGENCY REPORT NUMBER
41350.1-CH

11. SUPPLEMENTARY NOTES
The views, opinions and/or findings contained in this report are those of the author(s) and should not be construed as an official Department of the Army position, policy or decision, unless so designated by other documentation.

12 a. DISTRIBUTION / AVAILABILITY STATEMENT
Approved for public release; distribution unlimited.

12 b. DISTRIBUTION CODE

13. ABSTRACT (Maximum 200 words)

The chemistry of dimethyl methylphosphonate (DMMP), which is used as a simulant for organophosphorus nerve agents, is being studied on model systems consisting Ni and Cu nanoparticles supported on titania. On the small Ni particles and unannealed Ni films (50 monolayers), DMMP decomposes to produce CO and hydrogen as the main gaseous products, leaving atomic phosphorus on the surface. However, the reactivity of the large particles heated to 850 K and the annealed Ni films is dramatically decreased. This reduction in activity is not attributed to a particle size effect, but is believed to be related to changes induced by annealing. Defects, such as steps and kinks, in the unannealed Ni surface are likely to be lost after heating, and is it also believed that a TiO_x species migrates onto the Ni surface during heating and passivates the surface. On the Cu particles of different sizes and on a 40 monolayer Cu film, DMMP decomposition produced methane as the major gaseous product, with formaldehyde as a minor product. Although the large and small Cu particles did not exhibit significantly different reactivity, the production of formaldehyde increased with increasing Cu coverage.

14. SUBJECT TERMS

15. NUMBER OF PAGES

16. PRICE CODE

17. SECURITY CLASSIFICATION OR REPORT	18. SECURITY CLASSIFICATION ON THIS PAGE	19. SECURITY CLASSIFICATION OF ABSTRACT	20. LIMITATION OF ABSTRACT
UNCLASSIFIED	**UNCLASSIFIED**	**UNCLASSIFIED**	**UL**

Table of Contents

Statement of Problem Studied

This project involved the investigation of Cu and Ni nanoparticles supported on titania as model catalysts for the decomposition of chemical warfare agents. Specifically, dimethyl methylphosphonate (DMMP) was used as a nontoxic simulant molecule for understanding the chemistry of the highly toxic organophosphorus compounds. Although bulk transition metal surfaces have been shown to be effective in breaking P-C and P-O bonds in DMMP, atomic phosphorus is difficult to remove from the surface of the metal and poisons the system toward further DMMP decomposition. Since metal nanoparticles are known to exhibit chemistry different from that of their bulk metal counterparts, the chemistry of DMMP was studied on Cu and Ni nanoparticles with controlled sizes and size distributions. Furthermore, the interactions between the nanoparticles and the highly reducible titania support could play an important role in chemistry on the nanoparticle surfaces; for example, spillover of oxygen from the titania support to the nanoparticle surfaces could facilitate the removal of atomic phosphorus and carbon by oxidation to a gaseous CO_x or PO_x species. All experiments were carried out under ultrahigh vacuum conditions ($P \leq 2x10^{-10}$ Torr) in order to control the surface compositions on the atomic level, and surface analysis techniques such as scanning tunneling microscopy (STM), X-ray photoelectron spectroscopy (XPS) and temperature programmed desorption (TPD) were used to characterize nanoparticle sizes and surface chemistry.

Summary of Most Important Results

Overview

In order to study particle-size dependent chemistry, it was necessary to develop a protocol for preparing surfaces with a uniform size distribution of metal nanoparticles. For both Cu and Ni, uniform size distributions could be obtained by controlling the diffusion/flux ratio during deposition. The narrowest distributions could be obtained by using the lowest diffusion/flux ratio, and at room temperature, the diffusion of Cu and Ni are sufficiently slow such that a flux of ~0.5 ML/min produces a uniform size distribution of nanoparticles. Larger particles could be prepared by room temperature deposition followed by heating to elevated temperatures while maintaining the uniform size distributions.

The TiO_2 support surface itself was found to be active for DMMP decomposition although it was less active than both Cu and Ni nanoparticle surface. On TiO_2, DMMP decomposition produced gaseous methane and methyl radicals while phosphorus remained on the surface as a PO_x species. X-ray photoelectron spectroscopy studies demonstrated that DMMP decomposition occurred at room temperature on highly reduced TiO_2 surfaces but not on the more stoichiometric surfaces.

DMMP decomposition on the Cu nanoparticles was found to be insensitive to the size of the particles although the fraction of exposed titania surface was important in determining reaction chemistry. DMMP decomposition occurred at lower temperature on the Cu nanoparticles (room temperature) compared to on titania itself, and DMMP decomposition produced qualitatively different products. On the Cu surfaces, formaldehyde and methane were the major gaseous decomposition products although H_2 and methyl radical desorption were also detected. Formaldehyde appeared to be the product associated with reaction on Cu and methane with reaction on titania. This supports the idea that DMMP decomposition proceeds via a methoxide intermediate since methoxide on Cu is known to produce gaseous formaldehyde.

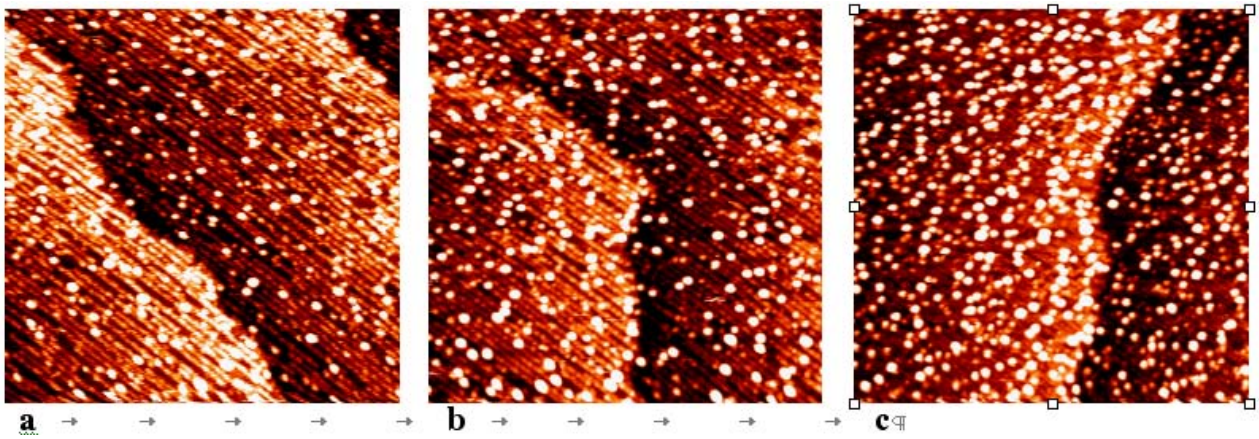

Figure 1. Scanning Tunneling Microscopy images of Cu nanoparticles deposited on the highly reduced titania surface at room temperature: a) 0.14 ML; b) 0.35 ML and c) 0.51 ML. All images are 1000Åx1000Å.

On the Ni nanoparticles, more extensive DMMP decomposition occurred at room temperature compared to reaction on the Cu nanoparticles or titania support surface. DMMP decomposition produced CO and H_2 as the main gaseous products, which is also consistent with methoxide as a decomposition intermediate since methoxide on Ni surfaces produces CO and H_2. Phosphorus remained on the surface in the form of atomic phosphorus rather than PO_x. DMMP chemistry was almost completely shut down on the larger Ni particles produced by heating to 850 K. However, the difference in chemistry was not attributed to a particle size effect. Instead, it is believed that the Ni particles become partially encapsulated with a reduced titania species upon heating, and this TiO_x passivates the active sites on the Ni particles. Lattice oxygen from the titania support was found to oxidize atomic carbon deposited on the Ni surfaces, but phosphorus could not be removed, even after heating in oxygen gas.

Characterization and Growth of the Cu and Ni Nanoparticles

Deposition of Cu on the reduced titania surface at room temperature resulted in relatively small particles with uniform size distributions.(see Figure 1, and Table 1). Cu growth on the reduced TiO_2 surface exhibits the same "self-limiting" growth observed on the (1x1) surface.[1] Specifically, Figure 1 shows that as the Cu coverage is increased, the particle density increases while the particle size remains approximately the same; moreover, each surface coverage exhibits a narrow size distribution. This growth behavior is markedly different from typical diffusion mediated growth, which is observed for the growth of metals on metals. For diffusion mediated growth, the particle density saturates at low coverages (<0.05 ML), and increasing the coverage results in increasing particle size so that the particles that nucleate first are always the largest.[2] Previous studies of titania surfaces prepared in vacuum have shown that these surfaces tend to be very defective compared to metal surfaces.[3-5] These defects are believed to be oxygen vacancies since the vacuum-annealed TiO_2 substrates are oxygen-deficient (reduced). Consequently the growth of metal nanoparticles on TiO_2 is not purely diffusion mediated, as it would be for the growth of metal particles on a metal surface. Instead these surface defects can act as sites that pin the diffusing metal atoms, and therefore the density of metal particles on the more defective surfaces is higher.

Table 1. Particle sizes and densities for various Cu coverages deposited at room temperature. The reported errors represent standard deviations.

Coverage (ML)	Average Height (Å)	Average Diameter (Å)	Particle density (cm^{-1})
0.14	4.9±1.1	23.0±3.0	$2.1x10^{12}$
0.35	5.5±1.3	26.6±2.9	$3.6x10^{12}$
0.51	5.3±1.0	24.7±3.2	$6.2x10^{12}$

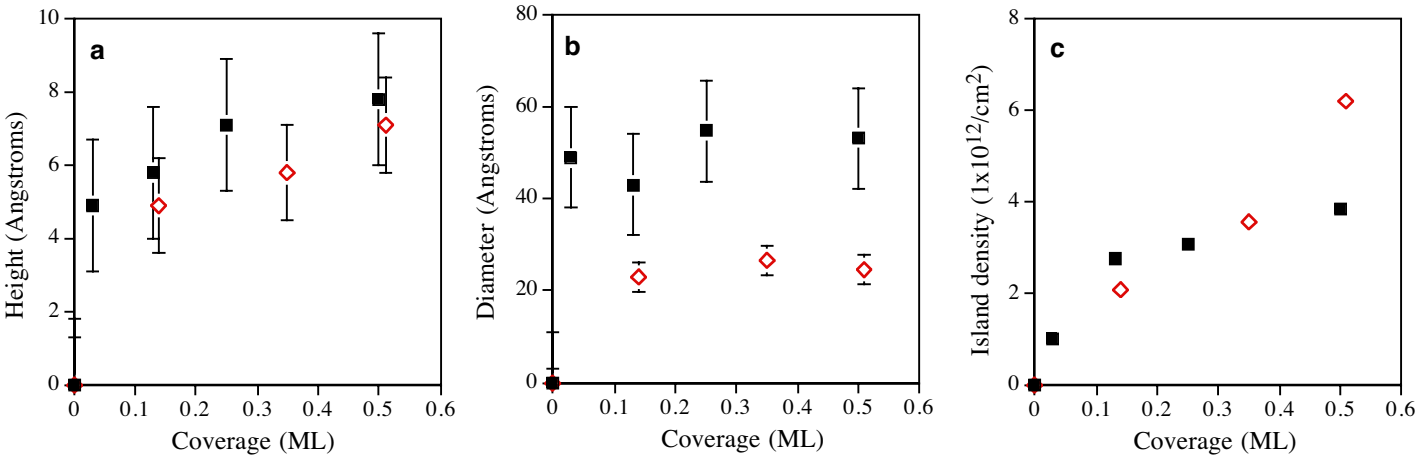

Figure 2. Size and particle densities of the Cu nanoparticles as a function of coverage. Data for Cu deposition on the highly reduced (1x2) surface is depicted by the solid squares. For the sake of comparison, data for Cu deposition on the more stoichiometric (1x1) surface is also shown (open diamonds).

We have estimated the Cu coverage in monolayers (ML) based on the average Cu particle size from STM images of the surface with the lowest coverage. Since the sizes of the nanoparticles particles are generally overestimated by STM due to tip convolution effects [1], the coverages that we report here represent an upper limit. For higher coverages we assumed that the Cu flux increases linearly with dosing time. One ML is defined by the packing density of the Cu(111) face.

The major differences between growth on the (1x2) vs. (1x1) surface are that the (1x2) surface produces smaller particle sizes (average diameter 23-27 Å vs. 50 Å, average height 5 Å vs. 6-8 Å) and greater particle densities ($6.2x10^{12}$ vs. $3x10^{12}cm^{-1}$).[1] Figure 2 graphically illustrates these differences as well as the self-limiting growth behavior on both surfaces. Remarkably, the particle density on the (1x2) surface does not appear saturate even at the highest coverage of 0.51 ML. We plan to conduct further studies to identify the coverage at which the particle density begins to level off. Since the (1x2) surface is more reduced that the (1x1), the (1x2) surface should be more defective due to a greater number of oxygen vacancies. Consequently, it is not surprising that a higher nucleation density is observed on the (1x2) surface, which has more defects that can potentially pin the diffusing Cu adatoms.

The Cu nanoparticles exhibit little or no preference for residing at the step edges, especially at low coverage. In contrast, Cu particles grown on the (1x1) surface preferentially decorate the step edges [1] at all coverages, presumably because the diffusing Cu adatoms nucleate at the highest coordination site on the surface. The increased particle nucleation on the terraces cannot be entirely attributed to the unusually wide terraces on our (1x2) surface (500-1000Å); although

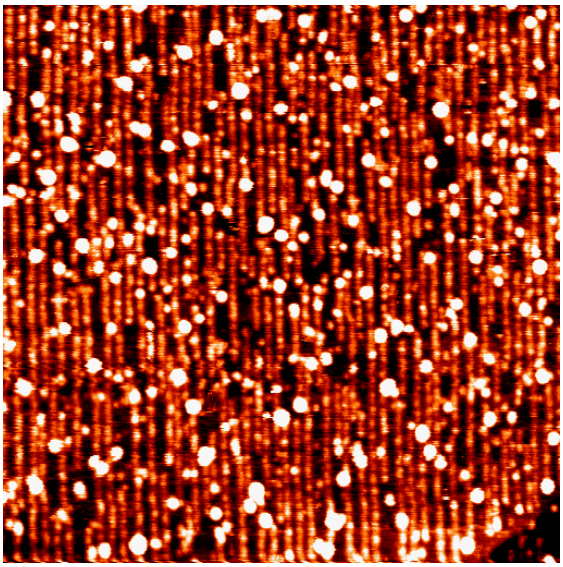

Figure 3. Scanning tunneling microscopy image of 0.14 ML of Cu on the TiO_2(110)-(1x2) surface, showing the preference for the nanoparticles to reside at the ends of the atomic rows. The image size is 1000Åx1000Å.

there are far fewer step edges than on the (1x1) surface, which has much narrower terraces (100-200 Å), the STM image in Figure 3 clearly shows that there are many Cu particles within 200 Å of a step edge. We believe that the lack of preference for the step edges on the (1x2) surface is very likely related to decreased mobility of the Cu atoms on this more defective surface. For the higher coverages, the Cu nanoparticles begin to aggregate in the vicinity of the step edges, but the particles reside on the upper terrace as opposed to straddling the step edges as they do on the (1x1) surface.[1]

Instead of preferential nucleation at the step edges, the STM images in Figure 3 suggests that Cu nanoparticles tend to reside at the ends of the bright rows associated with the (1x2) reconstruction. Similar nucleation behavior has been observed for Pt on reconstructed titania, and it is believed that the ends of these atomic rows consist of titanium atoms with lower coordination than the remaining (1x2) rows. Thus, the ends of the rows provide favorable high coordinate sites for the Cu adatoms.[6]

The size of the Cu nanoparticles could be increased annealing the surface to 700 K, following deposition at room temperature. As shown in Figure 4, the majority of the particles have an average diameter of 60-70 Å and height of 15-20 Å, and it is the particle density rather than average particle size that increases with increasing coverage. Consistent with the self-limiting growth observed at room temperature, the particle densities on the annealed surface increase with increasing coverage while the island sizes remain roughly the same. However, the particle size distribution is bimodal: the majority of the particles are considerably larger (60-70 Å diameter, 15-20 Å height) than those on the unannealed surface, but there are also some much smaller

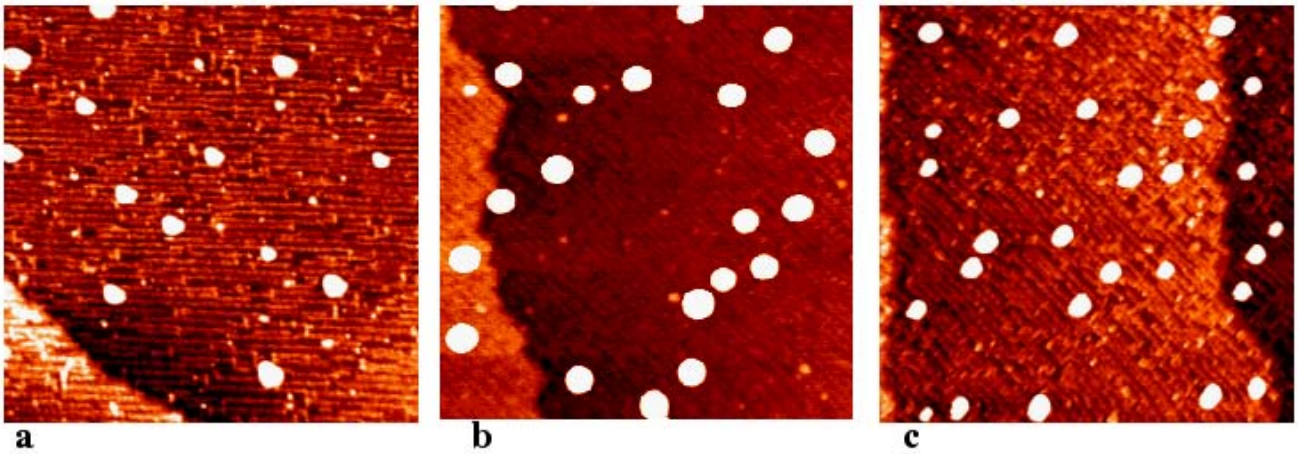

Figure 4. Scanning tunneling microscopy images of various Cu coverages deposited at room temperature and annealed to approximately 700 K: a) 0.14 ML; b) 0.35 ML; and c) 0.51 ML. All images are 1000Åx1000Å.

particles (~30 Å diameter, ~4 Å height). These smaller particles represent approximately 46% of the total number of particles at a Cu coverage of 0.14 ML, 38% at 0.35 ML, and only 10% at 0.53 ML. Since a uniform particle size distribution is required for our surface chemistry experiments, we will conduct further STM studies to establish whether the small particles can be completely eliminated at higher Cu coverages.

The growth characteristics observed on the (1x2) surface are all consistent with lower mobility of the Cu adatoms on the (1x2) surface compared to the (1x1), presumably due to the higher density of surface defects on the (1x2) surface. For example, the particle densities are greater on the (1x2) surface while the average particle size is smaller. Also, the annealed Cu particles are always located at step edges, which represent the highest coordination sites on the (1x1) surface. In contrast, there is no preference for the particles to be found at step edges on the (1x2) surface, which has a greater number of defects (other than step edges) that can potentially pin diffusing Cu adatoms.

In order to study particle size effects on surface chemistry, it is necessary to be able to prepare surfaces with uniform sizes distributions for a variety of particle sizes. Our previous studies of Cu particles on TiO_2(110)-(1x2) have shown that particles sizes, densities and size distributions can be controlled by the diffusion to flux ratio during deposition.[7] Specifically, when the rate of diffusion (D) is relatively slow compared to flux (F), the narrowest size distributions are obtained. Our current investigations of Ni growth on TiO_2(110)-(1x1) have demonstrate that the Ni particle sizes distributions can also be controlled via the D/F, as shown in Figure 5. When diffusion is infinitely slow compared to flux, there will be a uniform concentration of Ni atoms

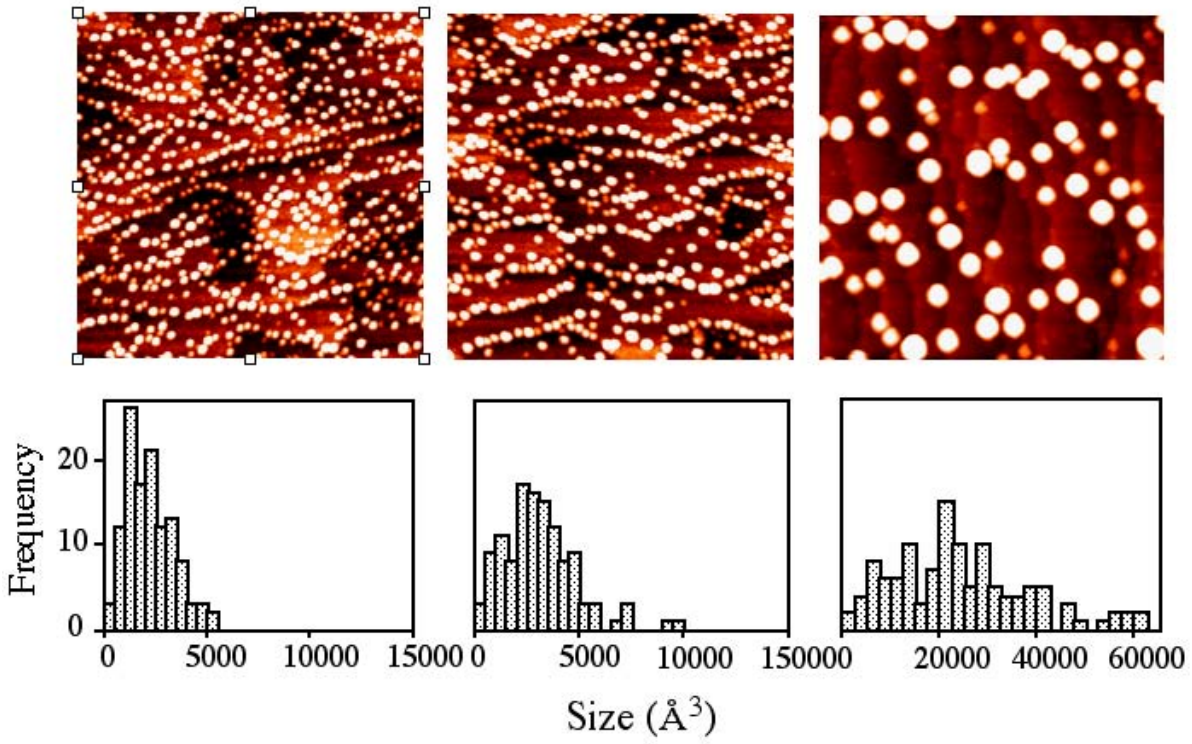

Figure 5. STM images and island size distributions for 1.0 ML of Ni deposited on TiO_2(110)-(1x1) under the following conditions: a) room temperature deposition, 0.16 ML/min; b) room temperature deposition, 0.02 ML/min; and c) 500 K deposition, 0.02 ML/min. Images sizes are 1000Åx1000Å.

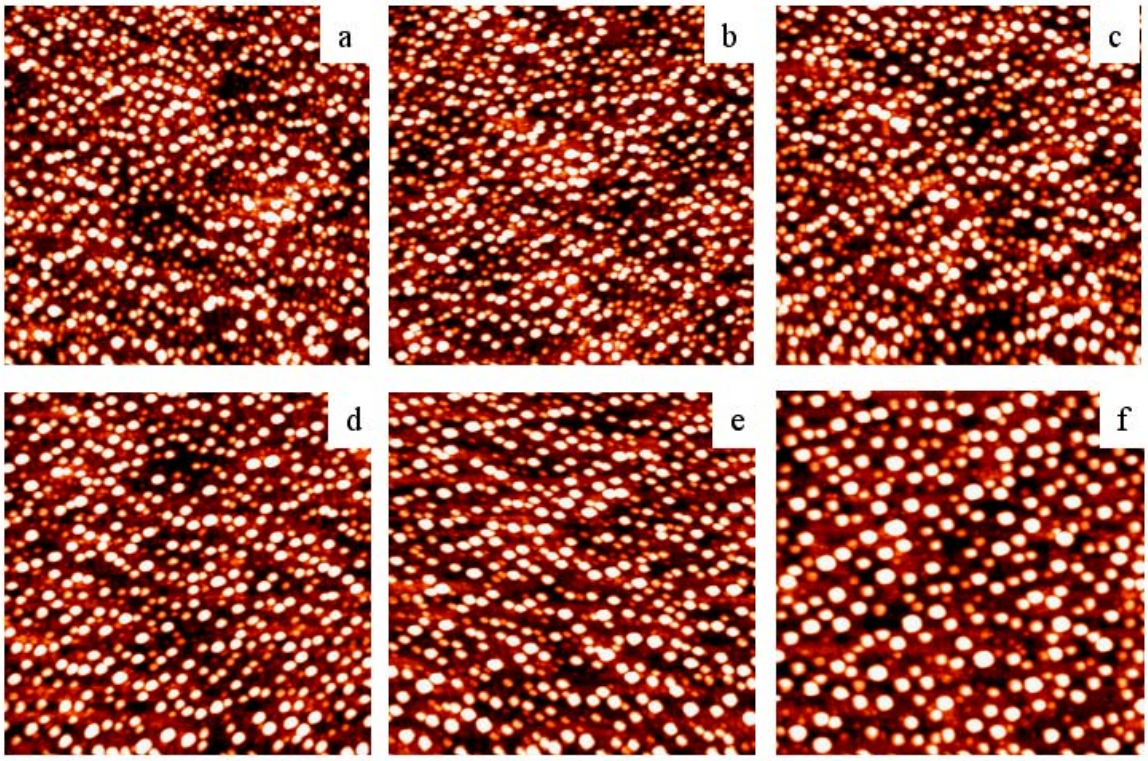

Figure 6. STM images of 2.5 ML of Ni deposited on TiO_2(110)-(1x2) at room temperature (a) and heated to the following temperatures: b) 400 K; c) 500 K; d) 700 K; e) 800 K; and f) 930 K. Images sizes are 1000Åx1000Å.

over the entire surface since the Ni atoms will remain where they land on the surface. When diffusion is slow compared to flux, the Ni atoms can only migrate short distances on the surface, and the concentration of Ni atoms is still quite uniform over the surface, resulting in islands that are all approximately the same size. The smallest D/F ratio corresponds to 295 K deposition at 0.16 ML/min, which yields the narrowest size distribution. Decreasing the flux to 0.02 ML/min causes the distribution to broaden slightly, while deposition at low flux and higher temperature (500 K) corresponds to the biggest D/F ratio and generates the broadest distribution. These results suggest that perhaps the D/F ratio may control the growth other metal islands deposited on oxide surfaces, provided that the metal island growth is 3-dimensional and the diffusion rate is relatively slow at room temperature. Notably, the growth of both Cu and Ni is qualitatively the same on the oxygen-deficient, reconstructed TiO_2(110)-(1x2) compared to the more stoichiometric, unreconstructed TiO_2(110)-(1x1) surfaces.

Island sizes for Ni deposited on titania can be controlled by the annealing temperature. When the islands are deposited at room temperature and then heated to elevated temperatures, a narrow size distribution is maintained, as shown in Figure 6. This is in contrast to deposition at elevated temperatures, which produces islands with very broad size distributions. As shown in Table 2, the sizes of the Ni islands do not substantially increase for annealing temperatures below 700 K. This behavior is different from that of annealed Cu islands, which grow in size above 400 K;[8] furthermore, the sizes of the Cu islands annealed to 800 K (98 Å diameter, 43 Å height) are much larger than the Ni islands annealed to the same temperature.[9] Our STM studies show that the slower growth of Ni islands upon annealing, or sintering (41.6 Å diameter,

Table 2. Average Ni particle dimensions as measured by STM for a 2.5 ML Ni coverage on titania, annealed to various temperatures. Measurements are for a set of at least 40 islands.

Temperature (K)	Average diameter (Å)	Average Height (Å)
295	34.0±5.9	9.1±2.1
400	34.2±5.5	9.2±2.3
500	35.8±6.5	9.6±2.2
700	38.0±7.3	10.3±2.8
800	41.6±6.2	9.9±2.4
930	50.3±9.1	14.6±5.4

9.9 Å height), can be attributed to the greater Ni-Ni (203 kJ/mol) bond strength compared to Cu-Cu (177 kJ/mol).[10] Larger islands are formed upon deposition at 500 K compared to deposition at room temperature followed by annealing for 1 hour at 500 K. This indicates that adatom detachment rather than adatom diffusion is the rate limiting step in island sintering for both Ni and Cu.[9]

DMMP Chemistry on Titania

TPD experiments for DMMP reaction on the TiO_2 surface demonstrated that methyl (15 amu, corrected for DMMP and methane cracking) is produced in a sharp peak at 700 K (Figure 7). Methane (16 amu) desorption is also observed in a broad feature with peaks at 435 K, 590 K and 700 K, while H_2 (2 amu) desorption occurs over the same temperature range but has no distinct peaks. The 15 amu peak at 700 K is assigned to methyl radical desorption since its intensity is too high to be accounted for by methane and DMMP cracking, and no higher masses are observed at this temperature. The desorption of molecular DMMP (79 amu) at 395 K and 585 K was also detected. The 79 amu signal is used to represent DMMP desorption since the parent mass signal at 124 amu has much lower intensity, and the cracking ratios for the 79, 94, 109 amu signals relative to 124 amu were identical to that of DMMP itself. The cracking pattern for DMMP in our mass spectrometer was determined by leaking DMMP directly into the chamber, and a wide mass scan from 1-100 amu indicated that there were no masses detected other than those associated with the cracking of DMMP. Specifically, the desorption of a phosphorus-containing species (31 amu) and the desorption of water (18 amu) were not observed. The amount of methyl radical production was highly dependent on the extent of TiO_2 reduction, with the more reduced surfaces producing more methyl radicals. The methyl radical yield was smallest on a new TiO_2 crystal that had been subjected to only a few sputter-anneal cycles. Furthermore, reoxidizing the reduced TiO_2 surface by heating in 1×10^{-6} torr of O_2 for an hour at 800 K also resulted in decreased methyl radical production.

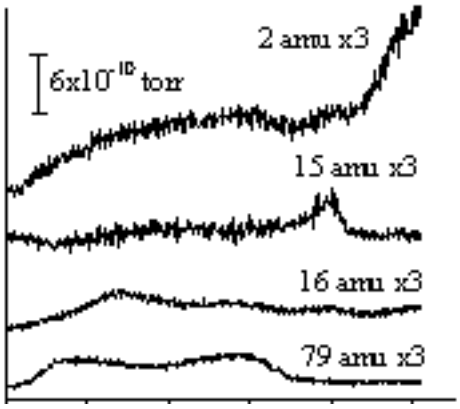

Figure 7. Temperature programmed desorption data for a saturation dose of DMMP adsorbed at 295 K and heated with a linear ramp of 2 K/s onTiO_2 (110).

XPS data for DMMP on TiO_2(110) after heating to various temperatures demonstrates that multiple carbon and phosphorus species exist on the surface during the thermal decomposition of

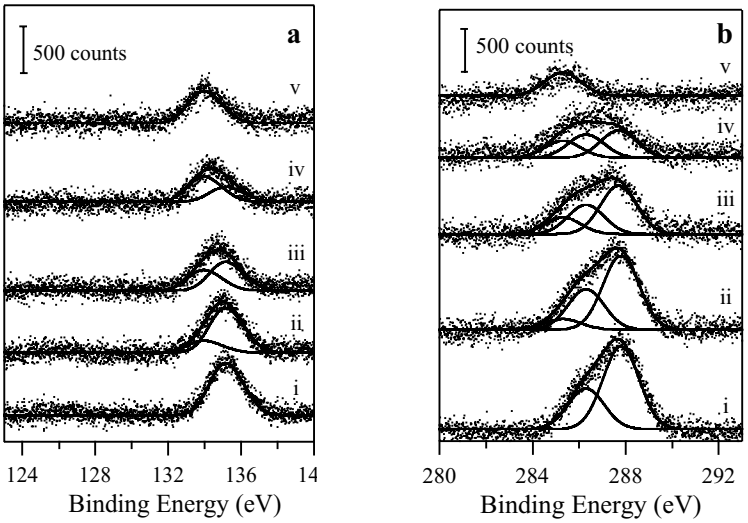

Figure 8. X-ray photoelectron spectra of the: (a) P(2p) and (b) C(1s) regions for a saturation dose of DMMP on TiO_2(110) at: (i) 295 K (no heating); and after heating to: (ii) 400 K; (iii) 550 K; (iv) 650 K; and (v) 850 K.

DMMP (Figure 8). TiO_2 was exposed to a saturation dose of DMMP at room temperature and then heated to 400 K, 550 K, 650 K, and 850 K with a linear temperature ramp of 2 K/s. The spectra shown in Figure 8 are nearly identical to those reported in an earlier study of DMMP decomposition on the more highly reduced TiO_2(110)-(1×2) surface.[11] Principal component analysis was used to establish that there were at least two linearly independent phosphorus-containing species and two linearly independent carbon-containing species on the TiO_2(110)-(1×2) surface between room temperature and 800 K, and the peak assignments described here are based on those for DMMP on TiO_2(110)-(1×2).[11] The main difference between DMMP reaction on the more stoichiometric (1×1) surface compared to the (1×2) is that the latter is slightly more reactive, and DMMP decomposition occurs even at room temperature. At room temperature, the P(2p) spectrum can be fit to a single peak at 134.9 eV, which has been assigned to phosphorus in molecular DMMP (Figure 8a). After the surface is heated to 400 K, a second P(2p) peak at 133.7 eV appears and is attributed to a PO_x species. As the surface is heated to higher temperatures, the 133.7 eV peak grows at the expense of the 134.9 eV peak, indicating DMMP decomposition, and only the 133.7 eV peak from PO_x is observed at 850 K. The phosphorus remaining on the TiO_2 surface could not be removed by further heating or by exposure to 1×10^{-6} torr of O_2 gas at 850 K for 40 minutes. The C(1s) spectrum of DMMP at room temperature consists of two peaks at 287.8 eV and 286.3 eV (Figure 8b). These two peaks are assigned to the methoxy and methyl carbons in molecular DMMP, respectively, and have the expected peak area ratio of 2:1. At 400 K, a small peak at 285.3 eV appears in addition to the two higher binding energy peaks and is assigned to a decomposition species such as CH_x or atomic carbon.[11] Upon further heating, the 285.3 eV species accounts for a greater fraction of the total surface carbon, and the single peak at 850 K is attributed to atomic surface carbon, given that all of the gaseous decomposition products have desorbed at this temperature.

DMMP Chemistry on Cu Nanoparticles

Scanning tunneling microscopy studies

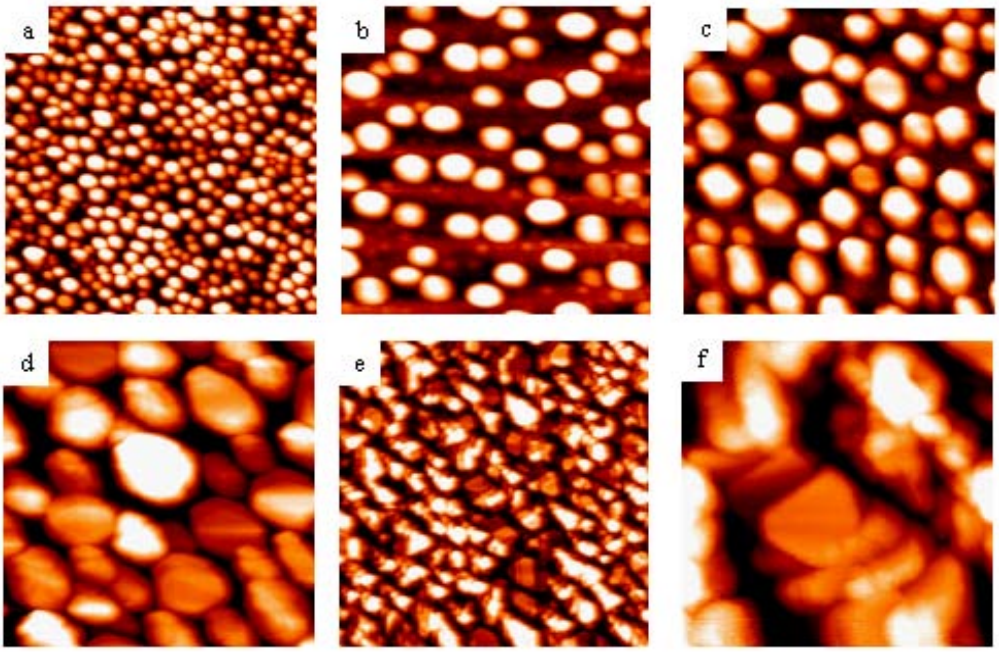

Figure 9. Scanning tunneling microscopy images of: (a) the small Cu clusters (6 ML) deposited at 295 K; (b) Cu clusters in (a) after DMMP reaction; (c) the large 20 ML Cu clusters (deposited at 295 K and annealed to 850 K); (d) the large 40 ML Cu clusters (deposited at 295 K and annealed to 850 K); (e) and (f) the 160 ML Cu film (deposited at 295 K and annealed to 850 K). All images except (e) are 100 nm×100 nm. The image size for (e) is 500 nm×500 nm.

In order to investigate cluster size effects for DMMP decomposition, different sizes of Cu particles as well as a Cu film were prepared by varying the coverage and the annealing temperatures after room temperature deposition. These Cu surfaces were the small Cu particles (6 ML) as deposited, the large Cu particles (20 ML and 40 ML) and the Cu film (160 ML). The large Cu particles and film were annealed to 850 K with a temperature ramp of 2 K/sec after room temperature deposition. All the Cu surfaces were imaged by STM after deposition, and their morphologies are shown in Figure 9. Deposition of 6 ML of Cu onto the titania surface at room temperature produced three-dimensional particles with an average diameter and height of 4.4±0.9 nm and 1.8±0.6 nm, respectively, based on the measurement of 40 particles (Figure 9a). During temperature programmed desorption experiments of DMMP, these Cu particles aggregated to form larger particles roughly 8.3 nm wide and 3.7 nm high (Figure 9b). Deposition of 20 ML Cu on titania followed by annealing to 850 K produced Cu particles with hexagonal shapes with diameters of 10.7 nm and heights of 4.8 nm (Figure 9c). 40 ML Cu deposited at 295 K and annealed to 850 K (Figure 9d) left 5% of the titania surface exposed and produced irregular Cu particles around 14.8 nm wide and 6.2 nm high. The large particles annealed to 850 K maintained their morphologies during DMMP decomposition. Although Cu particles covered the majority of the TiO_2 surface, approximately 5%~25% of the TiO_2 surface was exposed based on our surface area analysis of all the Cu surfaces. Integration of the STM images to determine the total surface areas has been described in a previous paper.[12] Figure 9e and 9f show the morphology of the Cu film prepared by depositing 160 ML Cu on titania and annealing the surface to 850 K. This film completely covered the substrate titania surface and was composed of irregular shapes of Cu domains. Although different deposition conditions produced various sizes of the Cu particles, the total surface areas of all the Cu surfaces studied before DMMP reaction were roughly the same.

Temperature programmed desorption studies

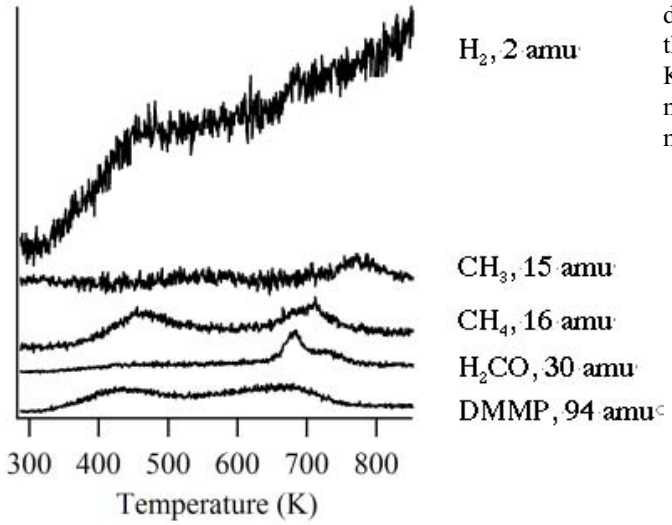

Figure 10. Temperature programmed desorption data for a saturation dose of DMMP adsorbed on the 40 ML Cu surface at 295 K and heated to 850 K with a linear ramp of 2 K/s. The spectrum for methyl radical is corrected for DMMP and methane cracking.

DMMP reaction on the 6ML, 20 ML and 40 ML Cu surfaces all produced same products: hydrogen (2 amu), methyl radical (15 amu), methane (16 amu) and formaldehyde (30 amu). The TPD data for DMMP decomposition on the 40 ML Cu surface is shown in Figure 10. The spectrum for methyl has been corrected for DMMP and methane cracking using a 1.4:1 ratio of methyl to DMMP (represented by mass 79) and a 0.89:1 ratio of methyl to methane. TPD data showed that the desorption peaks for H_2, methane and DMMP were very broad with the major

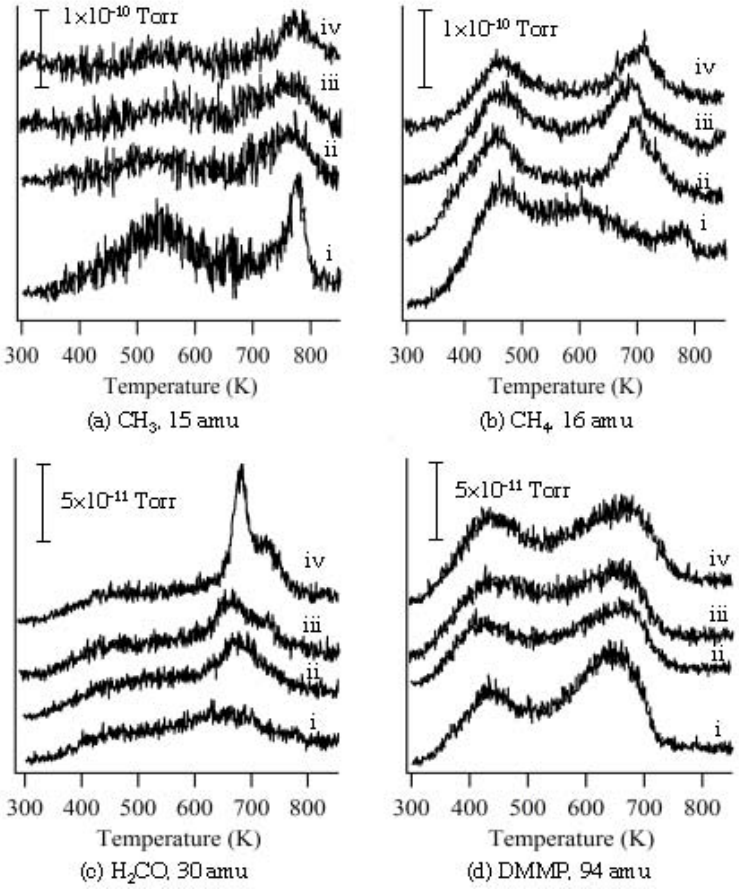

Figure 11. Temperature programmed desorption spectra for DMMP reaction on: (i) titania; (ii) the 6 ML small Cu particles; (iii) the 20 ML Cu surface and (iv) the 40 ML Cu surface.

features appearing at 460 K and 704 K for methane (16 amu) and 435 K and 670 K for DMMP (94 amu). Formaldehyde (30 amu) was evolved from the surface between 630 K and 785 K, with a distinct peak at 681 K. A small amount of methyl radical desorption was also observed at 777 K.

Comparisons of the production of methyl, methane and formaldehyde as well as molecular DMMP desorption on the titania surface and the Cu surfaces (6 ML, 20 ML and 40 ML) are shown in Figure 11. Methyl desorbed from the titania surface in two distinct peaks (540 K and 776 K), while methyl evolved from Cu surfaces at around 777 K. Furthermore, the formation of methyl on the Cu surfaces was 10-25% of that on the titania surface. Methane desorbed from all of the surfaces in a wide temperature range with peaks at 460 K and 704 K from the Cu surfaces and peaks at 460 K, 600 K and 776 K from the titania surface. Methane production from the 40 ML Cu surface was the smallest was 40% less than methyl production from the TiO_2 surface. DMMP decomposition on the titania surface did not produce formaldehyde. However, formaldehyde formation was observed on the 6 ML, 20 ML and 40 ML Cu surfaces between 630 K and 785 K, with a distinct peak at 680 K on 40 ML Cu surface. A similar amount of DMMP desorbed between 305 K and 755 K from all the surfaces studied.

X-ray photoelectron spectroscopy studies

XPS spectra of the C(1s) and P(2p) regions were collected after a saturation dose of DMMP on 3 ML Cu particles at room temperature (295 K) as well as after heating the surface to 400 K, 550 K, 660 K, 710 K and 850 K with a temperature ramp of 2 K/s (Figure 12). XPS data demonstrated that multiple carbon and phosphorus species existed on the surface during the thermal decomposition of DMMP.

As shown in Figure 12a, the P(2p) spectrum for DMMP adsorbed on the small Cu particles at room temperature can be fit with two peaks with binding energies of 134.9 eV and 133.7 eV. According to previous DMMP studies on the TiO_2(110) (1×1) and (1×2) surfaces, the phosphorus species at 134.9 eV was assigned to phosphorus in molecular DMMP adsorbed on titania, and the species at 133.7 eV was attributed to PO_x. Although molecularly adsorbed DMMP was the major species on the Cu particles at 295 K, 40% of DMMP already decomposed upon adsorption at room temperature, in contrast to the behavior on the TiO_2 surface. After heating the surface to 400 K, the total phosphorus signal was unchanged; however 55% of the DMMP decomposed, and the ratio of the two phosphorus species (134.9 eV: 133.7 eV) was 6:5. Heating to 550 K resulted in a loss of 20% of the initial phosphorus from the surface. The ratio of two phosphorus species (134.9 eV: 133.7 eV) was decreased to 5:12, and the 133.7 eV species (PO_x) was the dominant species present on the surface. The phosphorus signal decreased to 70% of its initial value upon heating to 660 K. Furthermore, a new peak accounting for 5% of the total phosphorus signal appeared at ~129 eV. This peak was assigned to atomic phosphorus on Cu, based on the 129 eV binding energy reported for atomic phosphorus on Rh.[13] The spectrum at 660 K can be fit with three peaks at 134.9 eV, 133.7 eV and 128.7 eV, which are assigned to DMMP, PO_x and atomic phosphorus on Cu, respectively, with PO_x accounting for 80% of the total signal. No molecular DMMP was present on the surface at 710 K, and PO_x accounted for 90% of the phosphorus signal. Although the total phosphorus signal remained the same after further heating to 850 K, 20% of the PO_x species was converted to atomic phosphorus. At 850 K, both PO_x and atomic phosphorus were present on the surface.

Consistent with previous DMMP studies on the titania surface, the C(1s) spectrum for DMMP on the small Cu particles (Figure 12b) at room temperature can be fit with three peaks at

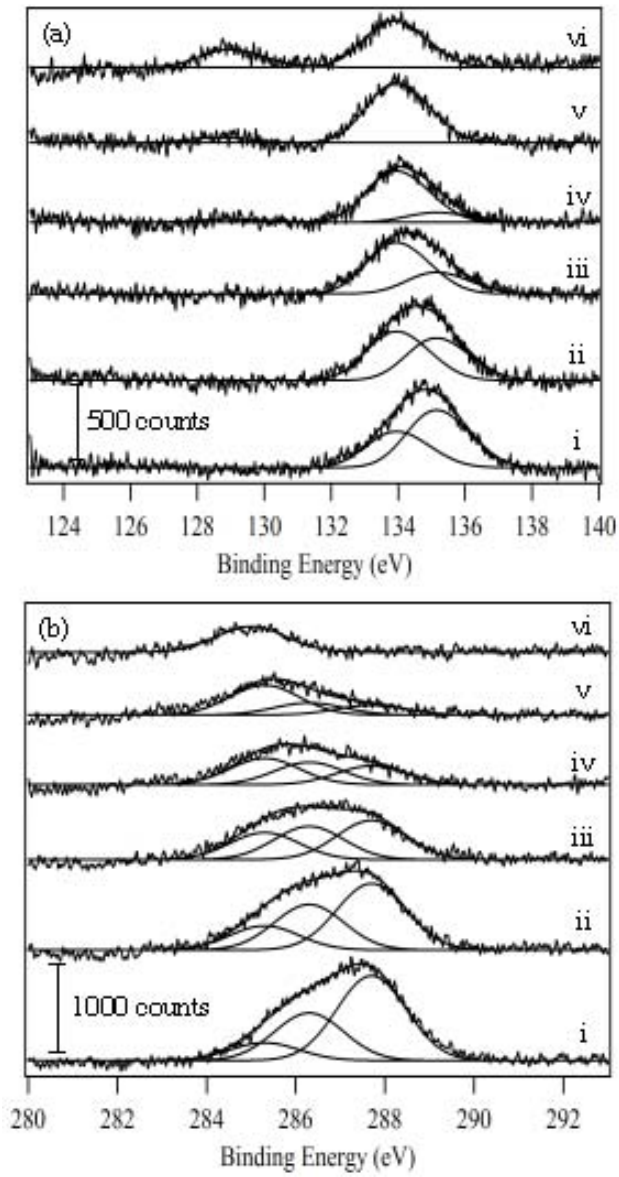

Figure 12. X-ray photoelectron spectra of the: (a) P(2p) and (b) C(1s) regions for a saturation dose of DMMP on the 3ML Cu particles at: (i) 295 K (no heating); and after heating to: (ii) 400 K; (iii) 550 K; (iv) 660 K; (v) 710 K and (vi) 850 K.

287.7 eV, 286.3 eV and 285.3 eV; these peaks are assigned to methoxy and methyl carbons in molecular DMMP as well as an atomic-like species such as CH_x, respectively.[11] The C(1s) spectra at 295 K confirms that DMMP decomposes at room temperature, as demonstrated by the significant intensity at 285.3 eV and the fact that the methoxy and methyl peaks from molecular DMMP peaks do not have a 2:1 area ratio. Distinct peak changes for the C(1s) spectra after heating to higher temperatures (Figure 12b) indicate that the relative intensities of the carbon species on the surface varied with temperature. At 850 K, approximately 20% of the initial carbon remained on the surface, and the spectrum is fit with a single peak at 285 eV. The species at 285 eV is assigned to atomic-like C on Cu since this peak is also present after DMMP decomposition on the Cu film, which completely covers the titania surface.

Based on the analysis of P(2p) and C(1s) peaks, DMMP decomposition on the Cu surface occurred immediately upon adsorption at 295 K, with molecular DMMP as the major surface species. Heating the surface to higher temperatures caused a decrease in carbon and phosphorus signal intensities due to the desorption of molecular DMMP and carbon-containing species (methyl, methane and formaldehyde). At 850 K, 70% of initial phosphorus as well as 20% of carbon is left on the surface. A comparison of DMMP reaction on Cu particles with that on Ni particles shows that Ni is more active toward C-P and O-P bond scission, and atomic phosphorus is left on the Ni surface at temperatures as low as 400 K. Only atomic phosphorus remainsed on the surface at 850 K. Although C-P and O-P bonds are broken on the Cu surfaces, atomic phosphorus does not appear until the temperature reaches 660 K, and PO_x is the major surface species even at 850 K.

Figure 13a shows the P(2p) regions after DMMP adsorption at room temperature on: titania, and coverages of 6 ML, 20 ML and 40 ML of Cu. The broadness of the P(2p) spectrum for the Cu surfaces suggests that some fraction of DMMP decomposed upon adsorption at 295 K to form PO_x. In contrast, the spectrum on the titania surface can be fit with a single P(2p) doublet corresponding to molecular DMMP. Based on the total integrated P(2p) signals, the relative

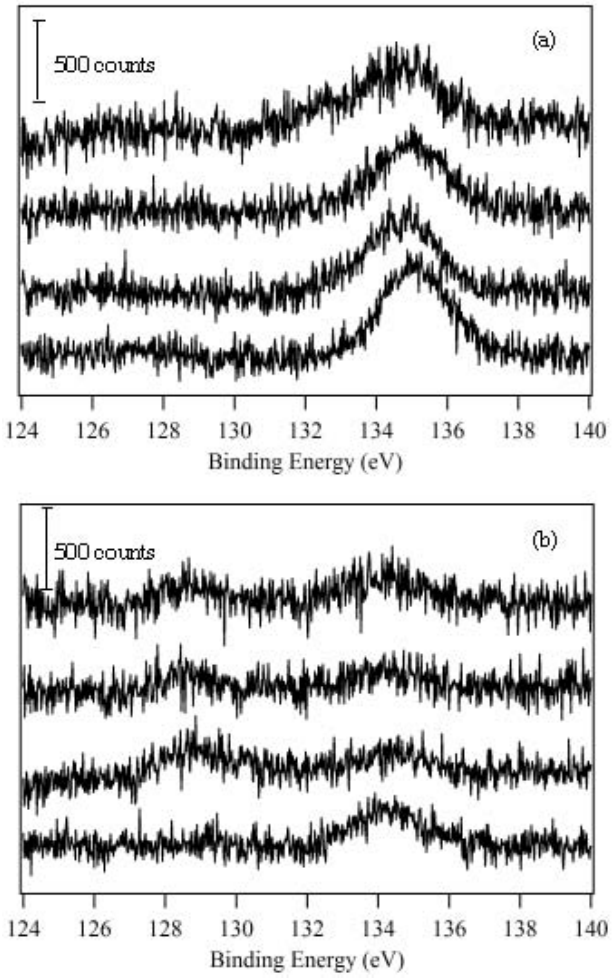

Figure 13. X-ray photoelectron spectra of the P(2p) region after a saturation dose of DMMP on: (i) titania; (ii) the small 6 ML Cu particles; (iii) the 20 ML Cu surface and (iv) the 40 ML Cu surface; at: (a) 295 K; and (b) after heating to 850 K.

saturation coverage of DMMP on these surfaces can be estimated. Roughly the same amount of DMMP is adsorbed on all the Cu surfaces, while DMMP adsorption is 20% higher on the titania surface. The C(1s) regions for DMMP adsorption at room temperature on all of the Cu surfaces (data not shown) confirms that DMMP immediately decomposes upon adsorption, resulting in a shift to lower binding energies compared with those on titania.

The P(2p) regions for DMMP heated to 850 K on the various surfaces are shown in Figure 13b. After DMMP decomposition, two main phosphorus species are present on all of the Cu surfaces. These species are assigned to atomic phosphorus on Cu at 129 eV and PO_x at 133.7 eV. On the titania surface only PO_x at 133.7 eV was observed. Given that phosphorus does not desorb from the surface, the amount of DMMP reaction can be estimated by dividing the integrated phosphorus signal after heating by the signal from DMMP adsorption at room temperature. The C(1s) spectra (data not shown) indicates that 10-15% of the original carbon signal was present after heating to 850 K.

Discussion

DMMP reaction on the Cu surfaces produced hydrogen, methane and formaldehyde as the major products and methyl radical as a minor product. PO_x, atomic phosphorus and carbon were left on the surface after the reaction. The XPS data indicated that DMMP decomposition on the Cu surfaces occurred immediately upon adsorption at 295 K. Heating the surface to higher temperatures resulted in a decrease in the phosphorus and carbon signals due to the desorption of molecular DMMP and carbon containing products (methyl, methane and formaldehyde). At 850 K, 30-50% of initial phosphorus and 20% of the initial carbon remained on the Cu surfaces.

The production of formaldehyde as a major product from DMMP reaction on the Cu surfaces suggests that methoxy is an intermediate species in DMMP decomposition. Previous studies of methanol oxidation on single crystal Cu surfaces demonstrated that methoxy is the intermediate species for the reaction, and the decomposition of the methoxy species forms formaldehyde and hydrogen at temperatures above 300 K.[12,14-17] A methoxy intermediate is also consistent with our previous studies of DMMP decomposition on Ni particles since methoxy is known to decompose to CO and H_2 on Ni surfaces.[18,19] Decomposition via a methoxy intermediate on

both the Cu and Ni particles explains the different gaseous products evolved from reaction on these two surfaces.

There was no apparent Cu particle size effect on the decomposition of DMMP observed in this study. From comparisons of DMMP reaction on the small Cu particles (6 ML, 4.4 nm in diameter, 1.8 nm in height) with that on the large Cu particles (20 ML, 10.7 nm in diameter, 4.8 nm in height), a similar amount of DMMP was adsorbed on both surfaces, and decomposition produced roughly the same amount of reaction products (hydrogen, methyl, methane and formaldehyde). The desorption of these products also occurred at the same temperatures. Compared with DMMP decomposition on Cu surfaces (6 ML and 20 ML), DMMP decomposition on the 40 ML Cu surface produced ~200% more formaldehyde, but 40%-50% less methane and methyl radical. The formaldehyde formation was increased by 360% on the 160 ML Cu film. The higher yields of formaldehyde on the 40 ML and 160 ML Cu surfaces cannot be explained by the Cu surface area or the total surface area (Cu and titania) since both of these areas were roughly the same for all the Cu surfaces. We propose that the lower production of formaldehyde on the 6 ML and 20 ML Cu surfaces is related to a greater surface area of bare titania. DMMP is known to adsorbed directly onto the titania surface in the cases where the Cu particles do not cover the entire surface. In fact, 20% more DMMP was adsorbed on the titania surface compared with that on Cu surfaces (6 ML, 20 ML and 40 ML) for a saturation dose of DMMP. Although all of the Cu surfaces had roughly the same Cu surface area, the deposition of 20 ML Cu on titania surface left 25% of the titania surface exposed. Initially, 10% of the titania surface was exposed after the deposition of 6 ML Cu at 295 K, but further heating of this surface during the TPD experiments resulted in 55% of the titania surface not covered by Cu. In contrast, the 40 ML Cu surface exposed only 5% of the titania surface, while the 160 ML Cu film completely covered the surface. While formaldehyde is produced from DMMP decomposition on the 160 ML Cu film, DMMP decomposition on titania produces methane and methyl instead of formaldehyde. Therefore, the lower production of formaldehyde on the 6 ML and 20 ML Cu surfaces could be attributed direct adsorption of DMMP on titania or migration of surface intermediates like methoxy from the Cu particles to the titania surface during heating. Previous experimental and theoretical studies of methanol on metals and oxides show that the methoxy intermediate are mobile at elevated temperatures.[14,20] This explanation is also consistent with the lower production of methyl and methane on the 40 ML Cu surface compared with that on the 6 ML and 20 ML Cu surfaces. With a greater fraction of the titania surface covered by Cu, the production of formaldehyde from DMMP decomposition becomes the dominant pathway.

Conclusions

The decomposition of DMMP on different Cu surfaces (6 ML, 20 ML, 40 ML and 160 ML) produced hydrogen, methane and formaldehyde as major reaction products, with PO_x, atomic phosphorus and carbon deposited on the surface. We propose that DMMP reaction on the Cu surfaces occurs via a methoxy reaction intermediate. Our studies indicate that DMMP chemistry is not sensitive to the size of the Cu particles. The decreased production of formaldehyde on small Cu particles compared to the Cu films is attributed to DMMP decomposition on regions of exposed titania and migrations of intermediates onto the titania surface.

DMMP chemistry on Ni nanoparticles

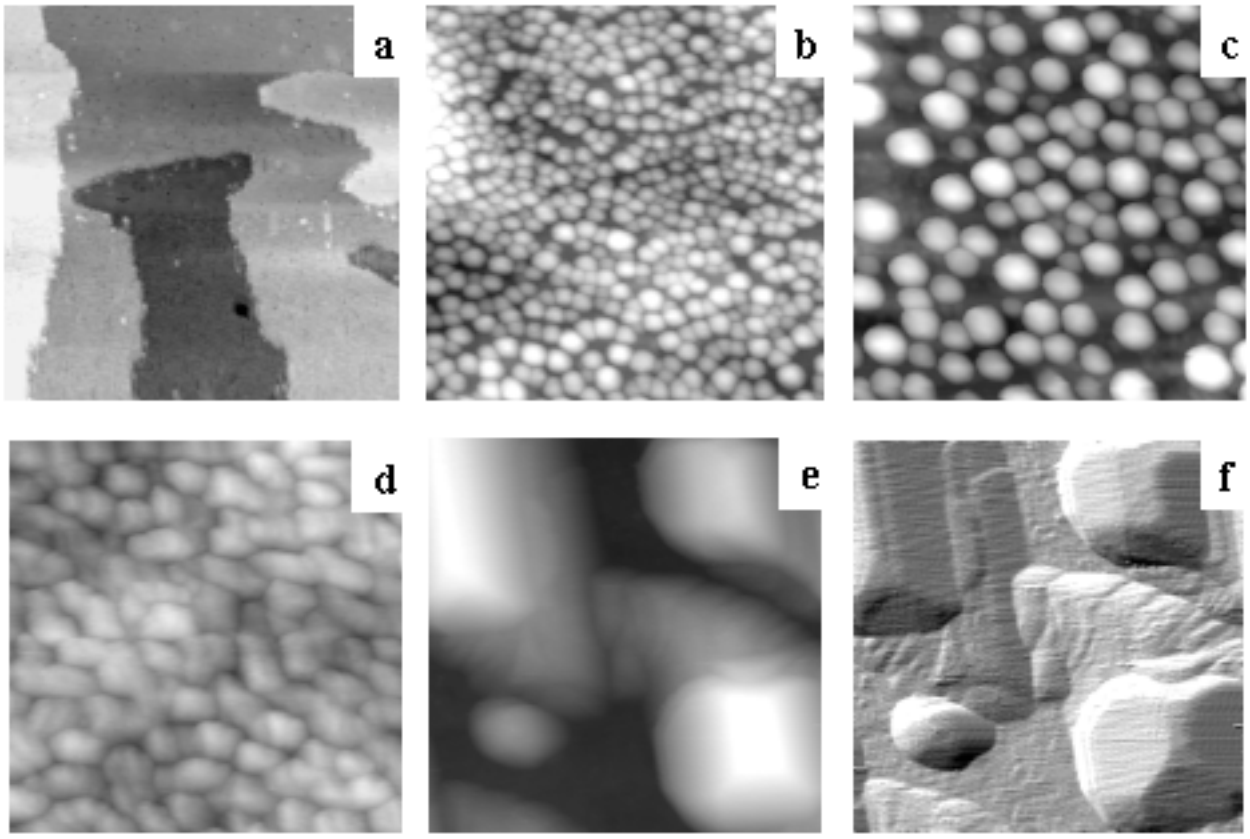

Figure 14 . Scanning tunneling microscopy images of: (a) TiO_2 (110); (b) the small Ni clusters (deposited at 295 K and flashed to 550 K); (c) the large Ni clusters (deposited at 295 K and annealed to 850 K); (d) the 50 ML Ni film deposited at 295 K; (e) the 50 ML Ni film deposited at 295 K and annealed to 850 K; and (f) the image in 1e differentiated in order to show the facets on the Ni islands. All images are 100 nm × 100 nm.

Scanning tunneling microscopy characterization of Ni nanoparticles

In order to investigate particle size effects on DMMP decomposition, different sizes of Ni clusters as well as Ni films were prepared and imaged by STM (Figure 14). The average sizes of the Ni clusters were determined from STM line profiles, but due to tip convolution effects, the measured diameters may be larger than the actual ones.[1,21] Figure 14 shows a sputtered and annealed TiO_2 surface consisting of 30-70 nm wide terraces, on which the bright atomic rows spaced by 0.65 nm are known to correspond to rows of Ti atoms.[22,23] Deposition of 3 ML of Ni onto this surface at room temperature and followed by quickly heating to 550 K produced three-dimensional clusters with a fairly uniform size distribution, as shown in Figure 14b. The average diameter and height of the clusters were approximately 5.0±0.8 nm and 0.9±0.2 nm, respectively, based on measurements from 20 clusters. Notably, the Ni clusters were initially heated to 550 K in order to remove any residual CO that was adsorbed during Ni deposition; however, residual CO adsorption was detected, and the morphology as well as surface chemistry of the Ni clusters were identical before and after heating to 550 K. Large Ni clusters with an average diameter of 8.8±1.4 nm and a height of 2.3±0.5 nm were prepared by deposition of 8 ML of Ni at room temperature followed by heating the surface to 850 K with a linear temperature ramp of 2 K/s (Figure 14c). Although the small and large Ni clusters covered the majority of the TiO_2 surface, the clusters left 15% and 30% of the TiO_2 surface exposed,

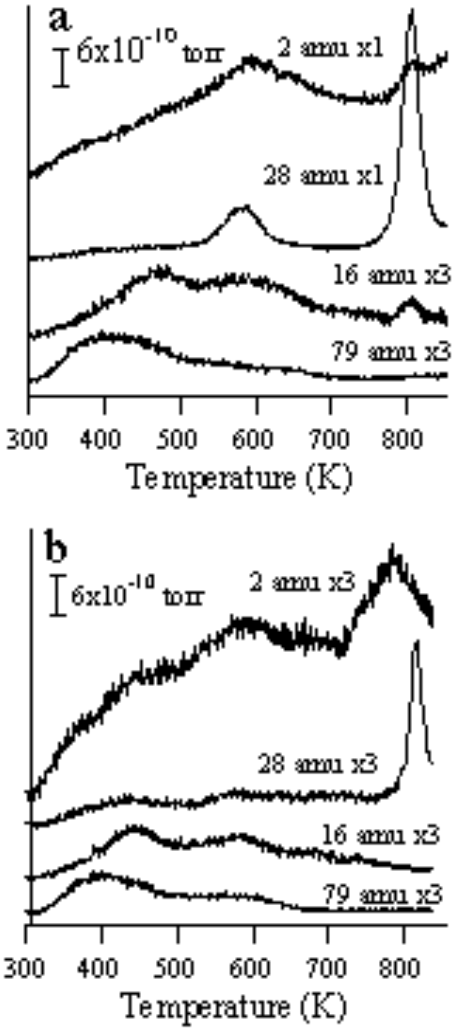

Figure 15. Temperature programmed desorption data for a saturation dose of DMMP adsorbed at 295 K and heated with a linear ramp of 2 K/s on: (a) the small Ni clusters; and (b) the large Ni clusters.

respectively. A Ni film that completely covered the titania surface was prepared by depositing 50 ML of Ni at room temperature (Figure 14d). Ni islands with an average width of 6.1 nm were observed, but the islands were irregularly shaped with no distinct facets. Heating this film to 850 K at 2 K/s produced large Ni islands roughly 30.0 nm wide and 13.2 nm high (Figure 14e). In addition to being much larger than the unannealed islands, these Ni islands had more regular shapes with facets that appear on the sides of the islands, as shown in the differentiated image (Figure 14f). Approximately 25% of the TiO_2 surface becomes exposed after annealing the 50 ML Ni film. During temperature programmed desorption (TPD) of DMMP, the large Ni clusters as well as the annealed Ni film maintained their morphologies because both of the surfaces had already been heated to 850 K. However, heating to 850 K caused the small clusters to aggregate into larger clusters (average diameter 5.5 nm, height 2.0 nm), and the unannealed Ni film formed large domains similar to the annealed Ni film in Figure 14e.

Temperature programmed desorption studies

DMMP reaction on the small 3 ML Ni clusters, which were deposited at room temperature and flashed to 550 K, produced CO (28 amu) and H_2 (2 amu) as the major products. CO desorption occurred in a large peak at 805 K and a smaller peak at 580 K (Figure 15a). The fact that the H_2 desorption peak at 580 K is larger than at 805 K suggests that the majority of DMMP decomposition occurs below 805 K. The main peak for DMMP desorption (79 amu) was at 400 K with a smaller shoulder at 630 K. Methane (16 amu) desorption occurred in a broad feature with distinct peaks at 470 K and 585 K; note that the 16 amu peak at 805 K is due to the cracking of CO. There is no evidence for methyl radical desorption, given that the 15 and 16 amu signals had exactly the same peak shape with approximately the correct 15:16 amu ratio for methane.

On the large Ni clusters (8 ML annealed to 850 K), DMMP decomposition resulted in the same gaseous products, but the yields of CO and H_2 were much lower than on the small Ni clusters (Figure 15b). On the large Ni clusters, CO (28 amu) desorption occurred at 815 K, and the lower temperature desorption peak was not detected. The main intensity for the H_2 signal appeared above 785 K, suggesting that most of the C-H bond breaking does not occur until high temperature. The desorption of DMMP (79 amu) and methane (16 amu) had roughly the same temperature profiles and intensities as those observed on the small Ni clusters except that the higher temperature DMMP peak was more distinct on the large Ni clusters. The intensity of the

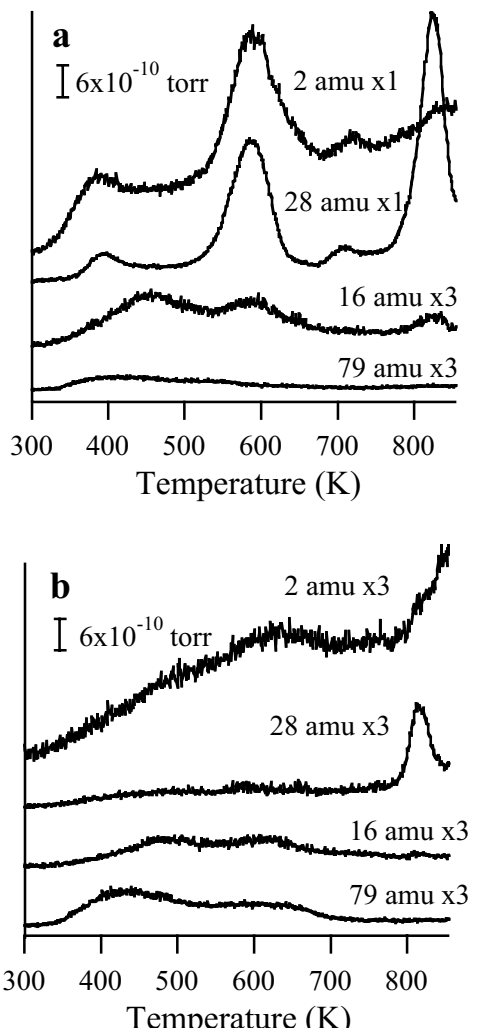

Figure 16. Temperature programmed desorption data for a saturation dose of DMMP adsorbed at 295 K and heated with a linear ramp of 2 K/s on: (a) the 50 ML Ni film deposited at 295 K; and (b) the 50 ML Ni film deposited at 295 K and annealed to 850 K.

high temperature CO peak was very sensitive to the level of reduction of the TiO_2 surface. On a more stoichiometric surface, the CO yield from the large clusters was 45% of that on the small clusters compared to 30% on the more reduced surface (Figure 15b).

DMMP reaction on a 50 ML Ni film deposited at room temperature resulted in large CO and H_2 desorption signals (Figure 16a). CO was produced in two large peaks at 585 K and 825 K, as well as two smaller peaks at 390 K and 705 K. Although the H_2 and CO signals had similar profiles below 800 K, the dominant peak in the CO signal occurred at 825 K, which corresponded to the smallest of the H_2 peaks. This behavior is again consistent with the majority of DMMP decomposition occurring below ~700 K. For the 50 ML Ni film annealed to 850 K before exposure to DMMP, very little CO and H_2 were detected in the TPD experiment (Figure 16b), suggesting that annealing the Ni surfaces decreases the activity for DMMP decomposition. The desorption profiles and intensities for DMMP and methane desorption were similar on the large Ni clusters and annealed Ni film, but the integrated intensity for DMMP desorption was almost 50% lower on the unannealed film. The lack of DMMP desorption is consistent with the large CO and H_2 signals and indicates that most of the adsorbed DMMP decomposes on the unannealed film. Annealing the 50 ML Ni film to 550 K before DMMP desorption did not change the chemical activity of the film.

In order to understand the role of oxygen from the titania support on DMMP decomposition, the TiO_2 surface was reoxidized with $^{18}O_2$ before deposition of the Ni clusters. The reoxidation treatment was carried out by exposing the TiO_2 surface to 1×10^{-7} torr of $^{18}O_2$ at 500 K for 30 minutes, followed by quickly heating to 800 K. For DMMP reaction on both the small and large Ni clusters, a high temperature peak around 805 -815 K was observed for the 30 amu ($C^{18}O$) and 28 amu ($C^{16}O$) signals. The 30 amu signal accounted for 60-70% for the CO desorption while the 28 amu signal accounted for 30-40%. On the small Ni clusters, the lower temperature 580 K CO desorption peak consisted only of 28 amu signal and had no contribution from 30 amu. There was no evidence for incorporation of ^{18}O into DMMP itself (126 amu) on either the small or large Ni clusters. The production of $C^{18}O$ from DMMP decomposition on the unannealed 50 ML Ni film provides further evidence that a significant fraction of titania becomes exposed after heating the film to 850 K during the TPD experiment.

X-ray photoelectron spectroscopy studies

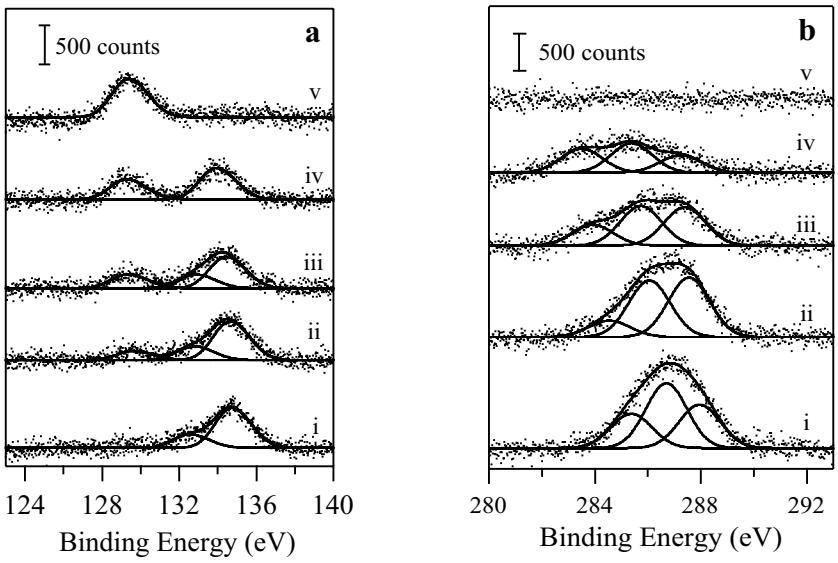

Figure 17. X-ray photoelectron spectra of the: (a) P(2p) and (b) C(1s) regions for a saturation dose of DMMP on the small Ni clusters (3 ML) at: (i) 295 K (no heating); and after heating to: (ii) 400 K; (iii) 550 K; (iv) 650 K;

As shown in Figure 17a, two peaks appear in the P(2p) spectrum for DMMP adsorbed on the small Ni clusters at room temperature, indicating that significant DMMP decomposition has already occurred upon adsorption, in contrast to behavior on the TiO_2 surface. The higher binding energy region can be fit with a peak at 134.5 eV, which is assigned to molecular DMMP based on a previous study of DMMP on Rh.[13] Notably the P(2p) binding energy for molecular DMMP on TiO_2 is slightly higher (134.9 eV) than that of DMMP on a transition metal surface. At 400 K, a new peak appears at ~129 eV and is assigned to atomic phosphorus adsorbed on Ni, based on the 129 eV binding energy reported for atomic phosphorus on Rh.[13,24] The spectrum at 650 K can be fit with two peaks at 133.7 eV and 129.1 eV with the former attributed to PO_x and the latter attributed to atomic phosphorus on Ni. After heating to 850 K, only atomic phosphorus on Ni is observed. The C(1s) spectra for DMMP on the small Ni clusters (Figure 17b) confirm that DMMP decomposes at room temperature, as demonstrated by the significant intensity at 285.3 eV and the fact that the methoxy and methyl peaks from molecular DMMP peaks do not have a 2:1 area ratio. The broadness of the C(1s) spectra even at room temperature reflects the presence of multiple carbon-containing species on the surface. Heating the surface above room temperature causes a change in the C(1s) peak shape as the lower binding energy peaks at ~283.5-284 eV appear. A comparison with the binding energy of atomic carbon on Ni(111)[25-27] suggests that atomic carbon is deposited on the Ni clusters. However, all of the carbon is removed from the surface after heating to 850 K.

A comparison of XPS data for DMMP adsorption at room temperature is shown in Figure 18 for the following surfaces: small Ni clusters, large Ni clusters, annealed Ni film and unannealed Ni film, and TiO_2. From the P(2p) data (Figure 18a), it is clear that the unannealed film is the most active for DMMP decomposition at room temperature since the 129 eV peak from atomic phosphorus on Ni is present. Furthermore, the small Ni clusters appear to be more active than all of the other surfaces with the exception of the unannealed film. The broadness of the P(2p) spectrum for the small Ni clusters suggests that there is more than one phosphorus species present, whereas the spectra on the titania surface can be fit to a single P(2p) doublet corresponding to molecular DMMP; the P(2p) spectra of the large Ni clusters and annealed Ni film have the main contribution from molecular DMMP. Based on the total integrated P(2p)

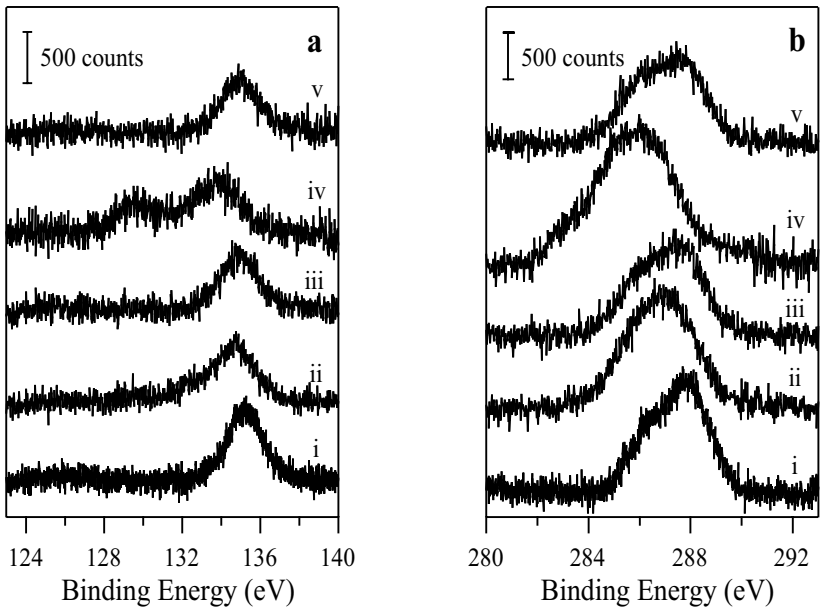

Figure 18. X-ray photoelectron spectra of the (a) P(2p) and (b) C(1s) regions after a saturation dose of DMMP at 295 K on: (i) TiO_2 (110); (ii) the small Ni clusters; (iii) the large Ni clusters; (iv) the 50 ML Ni film deposited at 295 K; and (v) the 50 ML Ni film deposited at 295 K and annealed to 850 K.

signals, the relative saturation coverages of DMMP on these surfaces were estimated. The TiO_2 and small Ni clusters adsorb roughly the same amount of DMMP, while adsorption is 20% less on the large clusters and annealed film, and 50% more on the unannealed film. Integrated intensities corresponding to the C(1s) region for DMMP adsorption at room temperature (Figure 18b) confirm the adsorption estimates from the P(2p) data. Again, the most DMMP decomposition is observed on the unannealed film, which has a C(1s) peak that is shifted to lower binding energy relative to the carbon species for molecular DMMP on TiO_2. This shift is also observed for DMMP on the small Ni clusters although it is less pronounced. For the annealed film and large Ni clusters, the C(1s) peak shape is more similar to that on the TiO_2 surface, where only molecular DMMP exists at room temperature.

XPS spectra for DMMP adsorption followed by heating to 850 K are shown in Figure 19 for the four Ni surfaces and TiO_2. On all of the Ni surfaces, the main phosphorus species is atomic phosphorus on Ni with a binding energy of ~129 eV (Figure 19a). However, a major difference is that almost no phosphorus remains on the annealed film and large Ni clusters while the phosphorus signal is significant on the unannealed film and small Ni clusters. Given that no phosphorus-containing species desorbs during heating, the amount of DMMP reaction on these surfaces can be estimated by dividing the integrated phosphorus signal after heating by the signal from DMMP adsorption at room temperature. In this manner, the percent reaction is calculated to be 85-90% on the small clusters and unannealed film, compared with 55-60% on the large clusters, annealed film and TiO_2 surface. The C(1s) data (Figure 19b) indicate that almost no carbon remains on the surface of the annealed film and large Ni clusters. While small carbon signals were observed on the small Ni clusters and annealed film, only the unannealed Ni film had a carbon signal that was significantly above the baseline.

Discussion

Small Ni clusters (5.0±0.8 nm diameter, 0.9±0.2 nm height) supported on TiO_2(110) are found to be more active for DMMP decomposition than large Ni clusters (8.8±1.4 nm diameter, 2.3±0.5 nm height), which were deposited at room temperature and annealed to 850 K. More DMMP decomposition occurs at room temperature on the small clusters compared to the larger ones. The greater activity of the small clusters is also reflected in the fact that nearly all of the

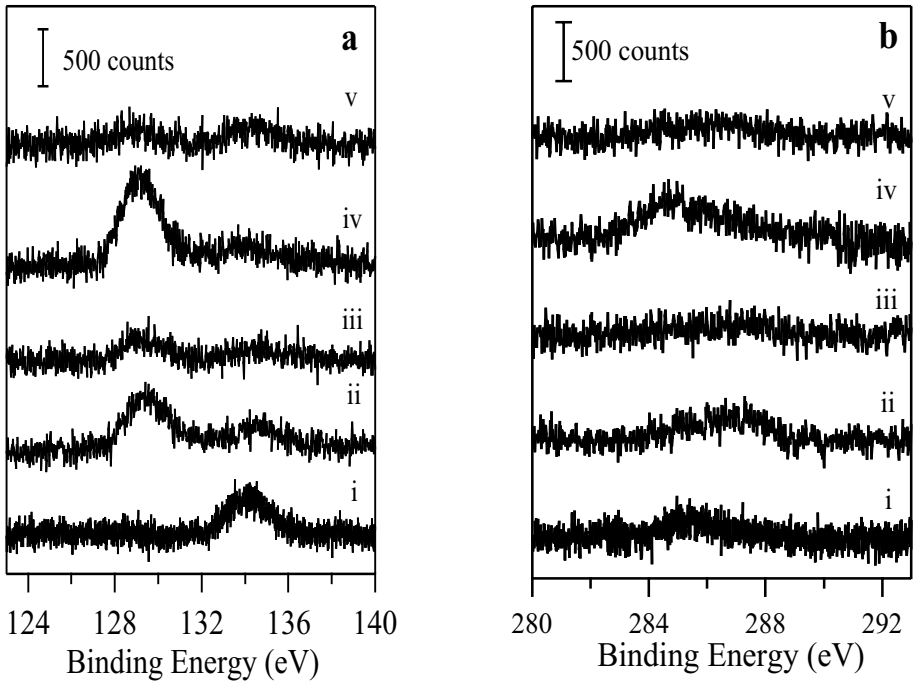

Figure 19. X-ray photoelectron spectra of the (a) P(2p) and (b) C(1s) regions after a saturation dose of DMMP followed by heating to 850 K at 2 K/s on: (i) TiO_2 (110); (ii) the small Ni clusters; (iii) the large Ni clusters; (iv) the 50 ML Ni film deposited at 295 K; and (v) the 50 ML Ni film deposited at 295 K and annealed to 850 K.

adsorbed DMMP decomposes on the small clusters, while only ~50% decomposes on the large clusters. DMMP decomposition and molecular desorption are competing processes on all of the Ni surfaces as well as the TiO_2 surface, and the amount of DMMP adsorption on the small and large clusters is comparable (within 20%). Notably, the TiO_2 surface itself has a DMMP saturation coverage similar to that of the small Ni clusters, and therefore DMMP adsorption is expected on exposed regions of the titania support as well as on the Ni clusters. The different sized Ni clusters have different reactivity, but this behavior does not appear to be caused by cluster size effects. Instead, the loss of chemical activity is attributed to the fact that the large clusters were annealed to 850 K whereas the small clusters were heated only to 550 K. Of the four Ni surfaces studied, the unannealed Ni film was the most active for DMMP decomposition, producing the greatest yields of CO and H_2 and leaving the most atomic phosphorus on the surface. DMMP reaction on the more ordered, annealed film produced CO desorption only at 815 K, and the saturation coverage of DMMP at room temperature was approximately half that on the unannealed film. Almost all of the DMMP adsorbed on the unannealed film is decomposed to produce atomic phosphorus, whereas only ~50% of the adsorbed DMMP is decomposed on the annealed film; this is consistent with the fact that much less DMMP is desorbed from the surface of the unannealed film.

The TiO_2(110) surface itself also decomposes DMMP, but titania is much less active than the small Ni clusters and produces significantly less H_2. Instead of decomposing DMMP into CO, as observed on the Ni surfaces, methane and methyl radical are the main carbon-containing products that desorb from TiO_2. On the Ni surfaces, approximately the same amount of methane is produced from DMMP decomposition as on TiO_2. However, methyl radical desorption is not observed from the Ni surfaces, presumably because Ni is more active for C-H bond breaking compared to TiO_2, and methyl intermediates would therefore be more likely to decompose to atomic carbon on Ni. The extent of methyl radical production is related to the level of reduction of the TiO_2 surface, with the more reduced surfaces producing the greatest methyl radical yield.

Other studies of chemical reactions on rutile TiO_2(110) have demonstrated that surfaces with a greater number of oxygen vacancies, which can be created either by annealing or by electron bombardment, are more chemically active.[28] For example, molecules such as O_2,[29] CO[30]formic acid[31] are more easily adsorbed on TiO_2 surfaces with oxygen vacancies. Oxygen vacancies also played an important role in the reactions of N_2O,[3,32] NO_2,[33] H_2O,[34] C_2H_2[3] and methanol[35] on TiO_2. Anatase TiO_2 surfaces that were sputtered to create more Ti^{+3} sites decomposed formic acid while the fully oxidized surfaces did not.[36]

Although the small Ni clusters and TiO_2(110) adsorb roughly the same amount of DMMP, decomposition occurs at room temperature on the Ni clusters while only molecular DMMP is observed on the TiO_2 surface. Furthermore, nearly all of the adsorbed DMMP reacts on the small Ni clusters after heating to 850 K, but only ~50% of the DMMP decomposes on TiO_2. Phosphorus remaining on the TiO_2 surface after DMMP decomposition is believed to contain intact P-O based on the 133.7 eV P(2p) peak in the X-ray photoelectron spectrum;[11] either the P-O bonds in DMMP are not broken on TiO_2 or atomic phosphorus binds to lattice oxygen on titania. In contrast, phosphorus remaining on the Ni clusters is assigned to atomic phosphorus on a metal surface based on the 129 eV binding energy. Although the sintering of the small Ni clusters leaves TiO_2 surface exposed after heating to 850 K, the absence of the 133.7 eV phosphorus species indicates that phosphorus is bound to Ni rather than TiO_2. This suggests that DMMP decomposition occurs preferentially on the Ni surface even when a significant fraction of the TiO_2 surface is exposed. Moreover, methyl radical production from the reaction on TiO_2 is not observed when the Ni clusters do not cover all of the TiO_2 surface.

Despite that fact that the Ni clusters shut down the reactivity of the TiO_2 support itself, the TiO_2 surface still plays an important role in the production of CO from DMMP decomposition on the Ni surfaces. When TiO_2 is reoxidized with $^{18}O_2$ before Ni deposition, DMMP decomposition on these surfaces produced $C^{18}O$ as well as $C^{16}O$ at 805-820 K; for the small Ni clusters, only $C^{16}O$ is produced at 580 K. These experiments confirm that the C-O bond in DMMP is broken, and the high temperature CO desorption involves the oxidation of atomic carbon by oxygen from the titania lattice. $C^{16}O$ desorption at 805-820 K may be attributed to atomic oxygen from the decomposition of DMMP, but this $C^{16}O$ desorption could also be due to oxygen from titania since the majority of the oxygen in the TiO_2 lattice is still ^{16}O. The absence of $C^{18}O$ desorption at 580 K on the small Ni clusters indicates that at these lower temperatures, either C-O bond scission in DMMP does not occur or oxygen from TiO_2 oxygen does not migrate onto Ni. The small or nonexistent carbon signals on the Ni surfaces after heating to 850 K are consistent with the fact that most of the deposited carbon is oxidized to CO. The decomposition of DMMP on the annealed 50 ML Ni films also results in the production of $C^{18}O$ at 815 K; since the annealed film consists of large three-dimensional islands with an average height of ~13 nm covering approximately 75% of the surface, the oxidation of carbon is expected to occur at the edges of the Ni-TiO_2 interface unless lattice oxygen is capable of diffusing over relatively long distances on the Ni islands. Oxygen migration onto the Ni surface is assumed rather than carbon migration onto TiO_2 because atomic carbon cannot be oxidized to CO on TiO_2 but can be oxidized on Ni surfaces. The higher desorption temperature of recombinant CO on the Ni clusters and films compared to on Ni(111) (805-820 K vs. 600 K)[37] can be understood in terms of the higher temperatures required for the diffusion of lattice oxygen. Other studies have shown evidence for interactions between surface intermediates and oxygen from the metal oxide surface. For example, carbon deposited from CO dissociation on

TiO_2-supported Rh clusters is oxidized by lattice oxygen from titania between 800 K and 1300 K to produce CO.[38] In the combustion of methane over Pd particles on alumina and zirconia, oxygen from the support is incorporated into the CO and CO_2 oxidation products.[39] O_2 is also known to dissociate on Pd clusters on TiO_2 and provide oxygen atoms that spill over onto the titania support.[40] Furthermore, the decomposition of formic acid on TiO_2(110) produces oxygen atoms that are incorporated into the titania surface.[41]

The decreased activity of the annealed Ni surfaces is *not* due to a loss of Ni surface area after annealing. The Ni surface areas for the clusters and films were calculated from the STM images using a Matlab program. All images were plane flattened before the surface area analysis. The STM images were collected at a resolution of 512×512 pixels, with each pixel representing a point in three dimensional space with an x, y and z coordinate. The projection of the STM image into the xy plane was divided into 511×511 squares, and each square was further divided into two triangles. The image surface area associated with each triangle was calculated using the x,y and z coordinates of vertices, from which the lengths of the sides of the triangle were determined. The total area of the imaged surface was calculated by summing the surface areas associated with the 522,242 triangles. The fraction of surface area covered by Ni was found by subtracting the surface area corresponding to regions of exposed TiO_2 from the total surface area. As shown in Table 1, the small and large clusters as well as the annealed Ni film have approximately the same Ni surface area despite the fact that the product yields of CO and H_2 on the small clusters are substantially higher. Estimates of the surface area of the Ni clusters from the cluster densities and average sizes of the clusters, which were assumed to have a paraboloid shape, are also consistent with the small and large clusters having the same surface areas. It is possible that the measured cluster sizes are overestimated due to tip convolution effects. Since tip convolution effects are more pronounced in the case of the small clusters, the calculated surface area of the small clusters would be overestimated compared to the large clusters and annealed film. Therefore, the lower activity of the annealed Ni surfaces cannot be due to reduced Ni surface area, which should be at least as great as the surface area of the small clusters. Furthermore, the small clusters actually sinter and lose surface area during the thermal decomposition of DMMP while the annealed clusters and film maintain the same surface area and morphology.

The amount of DMMP that adsorbs or reacts at room temperature on the Ni and TiO_2 surfaces can be discussed in terms of relative surface areas. The combined Ni and titania surface areas shown in Table 1 indicate that the Ni clusters and films have the approximately same total surface area, and the surface area of TiO_2 is ~15% lower. The TiO_2 surface and the small Ni clusters adsorb roughly the same amount of DMMP. However, the annealed Ni clusters and film adsorb ~20% less, providing further evidence for the lack of active sites on the annealed Ni surfaces. The unannealed Ni film adsorbs ~50% more DMMP even though the total surface area is approximately the same, and this result suggests that the increased activity of the unannealed film is due to a greater number of active sites.

Migration of a TiO_x moiety onto the Ni surface during annealing to 850 K could also explain the lack of activity for the annealed Ni surfaces. Our XPS experiments indicate that the titania surface becomes reduced after annealing an 8 ML Ni film to 850 K. A shoulder in the Ti(2p) spectrum (data not shown) appears around 456-457 eV and is assigned to Ti^{+3}.[4] It is not surprising that titania is reduced by the Ni clusters, given that previous photoelectron spectroscopy experiments[42,43] as well as theoretical studies[44] have shown that there are

electronic interactions between Ni clusters and the titania support. The initial deposition of the 8 ML Ni film does not result in a change in the Ti(2p) peak shape, indicating that titania is not reduced by deposition of Ni at room temperature. Moreover, annealing this Ni film to 600 K does not change the Ti(2p) peak shape. A slight shoulder around 456-457 eV first appears after heating to 700 K, and the intensity of the shoulder continues to increase after annealing to 800 and 850 K. Similarly, there is little change in the Ni(2p) intensity after annealing to 700 K although there is a ~0.1 eV shift to higher binding energy. Heating to 850 K causes a 20% drop in integrated peak intensity as well as +0.25 eV shift in binding energy compared to the Ni($2p_{3/2}$) position at room temperature. The loss of signal intensity is partially due to the agglomeration of the Ni film, which forms the large Ni clusters at 850 K. The slight shift in the Ni($2p_{3/2}$) position to higher binding energy may indicate that the Ni clusters have become oxidized, but shifts to higher binding energies have been also observed for supported metal clusters and films with increasing coverage and size.[45,46] It is possible that a reduced TiO_x moiety diffuses onto the Ni clusters during annealing since heating the deposited Ni to high temperatures is necessary to observe reduction of the titania support.

Investigations of Ni clusters supported on titania powders have reported that Ni clusters become encapsulated with TiO_x after heating to 773 K in a hydrogen atmosphere.[47-51] When Ni clusters on titania are reduced at high temperature, the capacity for CO and H_2 adsorption on these surfaces is diminished,[52-55] and this behavior has been described as a strong metal support interaction (SMSI). Transmission electron microscopy (TEM) studies have shown that titania-supported Ni clusters become covered with a species that was identified as Ti_4O_7 after reduction in H_2 at 1000 K.[56] The growth of TiO_x films on polycrystalline Ni surfaces decreases the capacity for CO and H_2 adsorption in a manner similar to the SMSI behavior.[55] In ultrahigh vacuum, other transition metal clusters such as Pt,[57-61] Rh[62-64] and Pd[40,65,66] deposited on TiO_2 are known to become encapsulated by TiO_x upon heating.[67,68] Studies of smaller Ni clusters (2-15 atoms) on TiO_2(110) by Anderson and coworkers have demonstrated that the Ni clusters become less active for CO adsorption after annealing to 600 K in ultrahigh vacuum.[69] Low energy ion scattering (LEIS) experiments showed that the Ni signal decreased upon annealing but did not disappear completely. Although the sintering of the Ni clusters could explain some of these effects, partial encapsulation of the Ni clusters could not be completely ruled out. Clusters consisting of only a few atoms are more likely to become encapsulated compared to the larger clusters and films investigated in this work, but Anderson and coworkers did not heat the supported Ni clusters above 600 K. Our studies have shown that heating the Ni clusters or the 50 ML film to 550 K also does not change the reactivity of the Ni surface whereas heating to 850 K shuts down chemical activity.

Another possible explanation for the reduced surface activity is that annealing causes a loss of defects, which are the active sites for DMMP decomposition. Freund and coworkers' investigations of alumina-supported Pd particles report that the particle surfaces are more defective than Pd(111) due to an increased number of step and edge defects.[70-74] Møller and Wu's infrared studies of CO adsorption on Ni films on TiO_2(110) show that CO adsorption on defect sites at the edges of Ni islands results in a ν(CO) frequency lower than that observed on (111) surfaces.[53] It is therefore reasonable to expect that the small Ni clusters and unannealed Ni film deposited at room temperature are also more defective than either single crystal Ni surfaces or Ni surfaces that have been annealed to 850 K. The paraboloid shapes of the small Ni

clusters as imaged by STM do not show any evidence of ordered structures. Although it is possible that the STM tip is not capable of resolving finer detail on this size scale, TEM studies by Tanner *et al.* also report that at low Ni coverages, the Ni clusters initially grow as small crystalline domes without any preferential orientation with respect to the titania surface.[75] The large clusters annealed to 850 K appear to have paraboloid shapes, but there is some evidence from the line profiles and STM images that facets are beginning to form in the larger clusters. The Ni film annealed to 850 K consists of large Ni islands with regular shapes as well as facets on the sides, in contrast to the unannealed film which is composed of irregularly shaped islands that have randomly grown together. The islands in the annealed Ni film are similar to the "hut-clusters" reported by Tanner *et al.* for annealed Ni islands on TiO_2[75]; the tops of the Ni islands have roof-like shapes, and the sides of the islands are inclined 35° from the plane of the titania surface. Tanner *et al.* concluded that the surfaces of the annealed Ni islands consist mainly of {111} and {100} facets.[75]

Although the unannealed clusters and films may be more defective than the annealed Ni surfaces, the absence of defect sites cannot completely explain the lack of reactivity for the annealed surfaces. The fact that four CO desorption peaks are observed for DMMP decomposition on the unannealed film suggests that there is more than one type of active site on this surface. Only two CO desorption peaks are observed for DMMP decomposition on the small Ni clusters, with the 580 K peak assigned to molecular desorption and the 805 K peak assigned to recombination of atomic carbon and oxygen. On the unannealed film, most of the CO intensity is also in the 580 K and 820 K peaks, but smaller desorption features at 400 K and 710 K appear. DMMP decomposition on the annealed film and clusters resulted in only one CO desorption peak around 815 K. Previous studies of DMMP decomposition on the Ni(111) surface show that CO and H_2 are produced with significant yields, and both the low and high temperature CO desorption peaks were observed.[37] Since the annealed Ni clusters and film must be more defective than the Ni(111) surface, the lack of CO production on the annealed surfaces cannot be solely attributed to the removal of defects in the Ni surfaces after heating. However, defects very likely play a role in the enhanced DMMP decomposition on the unannealed Ni surfaces; the 50 ML Ni film has only ~25% more surface area than the small clusters, but unannealed film produces twice as much CO from DMMP decomposition.

Since the desorption of CO from Ni surfaces has been well-studied in the literature, CO desorption experiments on the four Ni surfaces were carried out in order to better understand adsorption sites. To compare the total CO desorption yields on the four different Ni surfaces, these values were all normalized against CO desorption on the small Ni clusters (Table 1). CO desorption on the unannealed Ni film was three times higher than on the small clusters, while desorption from the annealed film and large clusters was only 30% of that on the small clusters. Although the annealed clusters and films should have less defective surfaces compared to their unannealed counterparts, the lack of surface defects cannot explain the decreased CO adsorption. Based on experiments reported in the literature, CO adsorbs strongly on the closed-packed Ni surfaces such as (111),[76-78] (110)[79] and (100).[80-83] In many of these experiments reported in the literature, CO was adsorbed at 100 K, whereas our experiments conducted on the Ni clusters and films involved adsorption at room temperature; however, the adsorption of CO on single-crystal surfaces at room temperature is known to be very similar to adsorption at low temperature,[84] and the sticking coefficient of CO on Ni(111) at room temperature is near unity.[85] CO should therefore adsorb equally strongly on the annealed Ni clusters and film,

which have surface structures similar to the close-packed faces of Ni. The lack of CO adsorption on the annealed Ni surfaces is further evidence that active sites become blocked by TiO_x or oxygen migrating from the titania support.

In terms of the catalytic decomposition of DMMP on TiO_2-supported Ni clusters, the Ni clusters are not ideal materials. Ni clusters and film deposited at room temperature have high activity for DMMP decomposition, but atomic carbon and phosphorus are deposited on the surface, which is passivated toward further reaction. Although carbon can be removed from the surface as CO above 805-815 K, heating to these temperatures will also cause the Ni surfaces to lose most of their activity. Furthermore, phosphorus cannot be easily removed from Ni surface even by treatment in oxygen at high temperature.[37] In any case, it is important to understand that the titania substrate is an active participant in the decomposition of DMMP, either by providing oxygen for the removal of surface carbon as CO or by possible migration of TiO_x onto the Ni surfaces.

Conclusions

The main gaseous products observed from DMMP decomposition on the Ni clusters and films (50 ML) are CO and H_2, and atomic phosphorus and carbon are deposited on the surface. However, carbon on the Ni surfaces is oxidized to CO above 800 K by oxygen from the TiO_2 lattice. Although the TiO_2 surface itself is capable of decomposing DMMP to methyl radicals, methane and H_2, the Ni clusters and films are more active for DMMP decomposition at room temperature. Small Ni clusters on TiO_2(110) were more active for DMMP decomposition compared to the large annealed Ni clusters, but this difference in chemical activity is not attributed to a particle size effect. Since the Ni film deposited at room temperature was also found to be more active than the annealed films, the loss of activity is attributed to changes that occur during the annealing process. Diffusion of a TiO_x species onto the Ni surfaces explains both the lack of DMMP decomposition and the lack of CO adsorption on the annealed surfaces.

The Comparison of Bacterial spores filtered across Anodiscs coated with Gold versus Copper

Experimental

Endospores of Bacillus subtilis strain PS832 were prepared at 24 ^{o}C in 2xSG medium. Although strain PS832 is a prototrophic derivative of strain 168, the most commonly used laboratory stain, DNA sequencing demonstrates negligible differences between the two strains. The PS832 endospore preparations were cleaned by repeated suspension in water followed by centrifugation until the preparations were free of sporulating cells, germinated spores or cell debris (>95%) as determined by phase contrast microscopy. These spores were then lyophilized and stored dry.

A stock spore suspension was prepared by mixing 21.2 mg of the spore preparation with 50 mL of deionized ultrafiltered water (DIUF) (Fisher Scientific, Fairlawn, NJ). The solution was prepared in an amber bottle and was stored at 5 ^{o}C. Before filtration the solution was sonicated for 15 min and then 0.5 mL solution was removed and mixed with 0.5 mL of DIUF water. This 1 mL solution was sonicated for 15 min, and then diluted to 50 mL with DIUF water and then sonicated for 15 additional min in order to minimize spore aggregation. Following sonication, the spores were filtered through Au or Cu coated Anodiscs™ (Whatman, Fisher Scientific).

The Anodiscs™ used were 47 mm in diameter with a nominal 0.2 μm pore size. Gold coated Anodiscs™ were prepared by coating with an Au layer having a thickness of ~100 nm using a

CrC-100 sputtering system (Plasma Sciences Inc., Lorton, VA). Copper coated Anodiscs™ were prepared by evaporating an Cu layer having a thickness of ~100 nm in an oil-free, home-built vacuum chamber. The base pressure was always 7 x 10^6 Torr or less. The chamber was initially roughed down by a Varian SH-100 scroll pump and was brought to the desired pressure by a Varian-V 70D turbopump. Cu was evaporated from a molybdenum boat by applying a DC voltage (~6.7V) consistent to apply a current of 200A for 15 seconds.

The filter membranes were transferred to a vacuum filtration system with a holder for 47 mm filters (Fisher Scientific). To the vacuum filtration system was added the bacterial spore suspension; the suspension was allowed to settle for approximately 30 seconds until the suspension ceased visibly moving. Vacuum filtration was then applied in order to achieve even distribution of individual spores throughout the surface of the Anodisc™. After filtration, the disks were transferred to a sample compartment supplied with dry purge air and allowed to dry overnight. Two bacterial spore filtration disks were prepared, one Au and one Cu coated, using the same volume of the same stock suspension, following the above method in order to examine the disk-to-disk variability. Also one-half of each spore filtration disk was heated in a 120 ^oC oven for 30 minutes to examine the dry heat disk-to-disk variability.

The bacterial spore disks were placed onto an aluminum microscope slide adjacent to a gold mirror for background measurements. Mid-infrared spectra were collected from 650-4000 cm^{-1} using a Nexus 470 FT-IR spectrometer coupled with a Continuμm microscope, both obtained from Thermo Nicolet (Madison WI). The FT-IR microscope was fitted with a liquid nitrogen cooled MCT-A (mercury-cadmium-telluride) detector, and the area sampled by the adjustable rectangular aperture was set to 100 x 100 _m ^{2} for the collection of *B. subtilis* spore spectra. Interferograms were apodized with a triangular function. Data was collected with the FT-IR microscope in reflectance mode and were recorded in absorbance units with 8 cm^{-1} resolution. A background spectrum was obtained immediately before each sample spectrum by positioning the X-Y microscope stage to a region on the gold mirror. Five spectra of each bacterial spore disk sample were collected, with 32 interferograms co-added and averaged, ensuring the microscope stage was positioned in different spots between each measurement.

Results

For comparison, the five sample spectra of B. subtilis spores filtered across each Anodiscs were averaged to give one representative spectrum for each of the disk samples; untreated and heated Au and Cu disks (Figure 20). The first method employed to determine the difference, if any, between Au and Cu, heated and untreated disk samples was to compare the scattering baselines of their averaged spectra. First, the spectral data was imported into Matlab (version R12 Mathworks Inc. Cambridge Ma.). The spectral regions of no absorbance attributed to spores were marked (Figure 21). These included the following spectral regions; 1800-2400 cm^{-1} and 3700-4000 cm^{-1}. Two additional spectral points were selected at 900 cm^{-1} and 680 cm^{-1} and a fifth order polynomial fit was made for the selected data for each sample. From each sample the corresponding polynomial was subtracted to yield a baseline corrected spectrum (Figure 22).

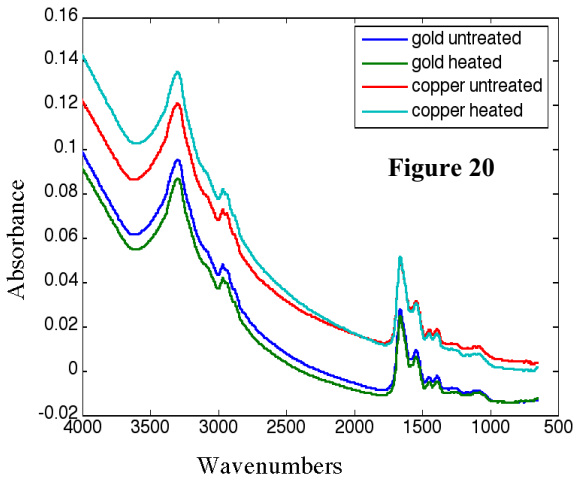

Figure 20

There was no significant differences observed between these baseline corrected spectra.

A Rayleigh scattering model of the loss of light due to scattering was examined as a second method undertaken to determine if there were spectral differences in the disk samples. In this case, the loss due to scattering is expected to be given by:

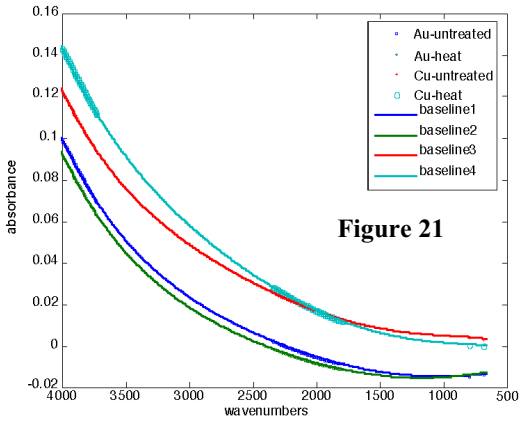

Figure 21

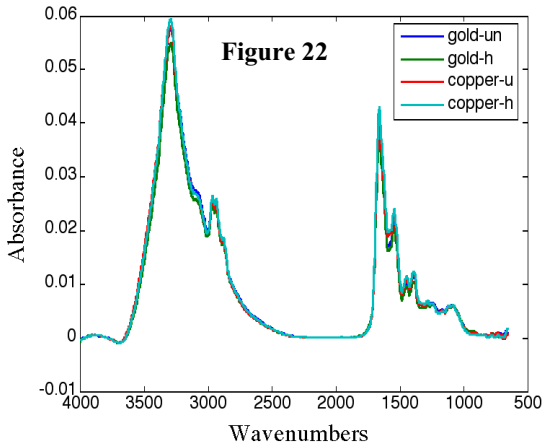

$$1.\quad \frac{I_s}{I_i} \propto \frac{1}{\lambda^4}\left|\frac{n^2-1}{n^2+2}\right|^2$$

where n is the complex refractive index and λ is the wavelength. Due to the Kramers-Kronig dispersion relation between the real and imaginary components of refractive index, the real index is approximately constant in the regions of the spectrum that do not exhibit absorbance. A plot of the loss (calculated as 1 minus reflectance) as a function of reciprocal wavelength to the fourth power (Figure 23) shows two significant linear regions, one above and one below the frequencies of the strong C-H and N-H absorbances in the spectrum. This suggests that a Rayleigh scattering model is adequate to describe these data even in the highest-energy portion of the mid-infrared spectrum near 2.5 micrometers wavelength. The slopes of the two linear regions then provide information on the relative magnitudes of the real refractive indexes of *B. subtilis* spores in the two regions. In the lower wavelength region, the slopes of the four samples were consistent with one another, 8.903 +/- 0.368. However, in the higher wavelength region, the heated copper sample had a higher slope compared to the other three samples (Figure 24). It was noted that this sample, following heating appeared discolored. This was most likely due to the formation of a Cu oxide layer. Thus the higher slope in the scattering model suggests that some light may be absorbed in this oxide layer and cannot be accounted for in the model.

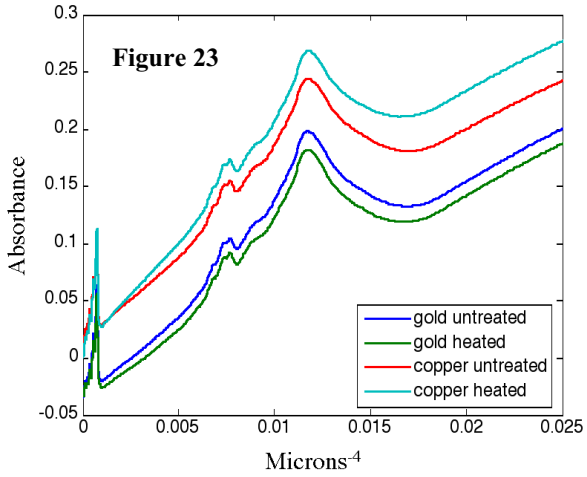

Conclusions

There are no significant differences in spectral properties of B. subtilis spores filtered across Anodiscs coated with Au or Cu, heated or untreated, as measured by FT-IR reflectance microspectroscopy. The only difference observed by baseline correction and Rayleigh scattering

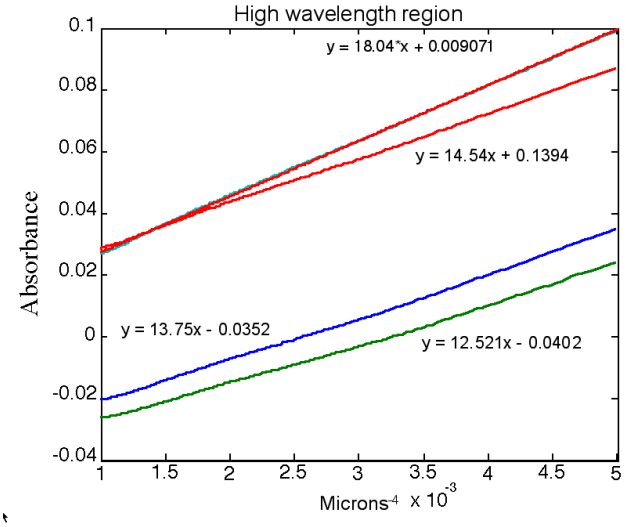

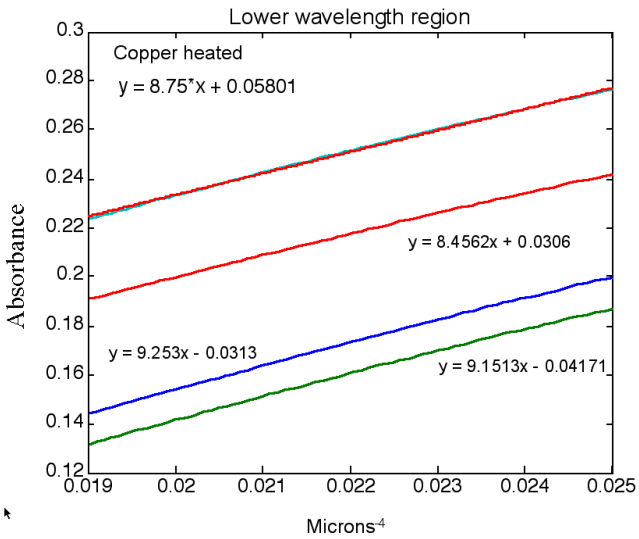

methods used in this study, was the heated copper coated Anodisc samples showed higher slopes in the Rayleigh models in the higher wavelength region.

References

[1] D. A. Chen, M. C. Bartelt, K. F. McCarty and R. Q. Hwang, *Surf. Sci.*, **2000**, 450, 78.
[2] M. C. Bartelt and J. W. Evans, *Surf. Sci.*, **1993**, 298, 421.
[3] G. Lu, A. Linsebigler and J. T. Yates, *J. Phys. Chem.*, **1994**, 98, 11733.
[4] J. M. Pan, B. L. Maschhoff, U. Diebold and T. E. Madey, *J. Vac. Sci. Technol. A*, **1992**, 10, 2470.
[5] L.-Q. Wang, K. F. Ferris, J. P. Winokur, A. N. Shultz, D. R. Baer and M. H. Engelhard, *J. Vac. Sci. Technol. A*, **1998**, 16, 3034.
[6] S. Gan, Y. Liang, D. R. Baer and A. W. Grant, *Surf. Sci.*, **2001**, 475, 159.
[7] J. Zhou and D. A. Chen, *Surf. Sci.*, **2003**, 527, 183.
[8] S. Ma, J. S. Ratliff, J. Zhou and D. A. Chen.
[9] J. Zhou, Y. C. Kang and D. A. Chen, *Surf. Sci.*, **2003**, 537, L429.
[10] D. R. Huntley, *J. Phys. Chem.*, **1989**, 93, 6156.
[11] J. Zhou, K. Varazo, J. E. Reddic, M. L. Myrick and D. A. Chen, *Anal. Chim. Acta*, **2003**, 496, 289.
[12] J. Zhou, S. Ma, Y. C. Kang and D. A. Chen, *J. Phys. Chem. B*, **2004**, in press.
[13] R. I. Hegde, C. M. Greenlief and J. M. White, *J. Phys. Chem.*, **1985**, 89, 2886.
[14] S. M. Francis, F. M. Leibsle, S. Haq, N. Xiang and M. Bowker, *Surf. Sci.*, **1994**, 315, 284.
[15] M. Bowker and R. J. Madix, *Surf. Sci.*, **1980**, 95, 190.
[16] I. E. Wachs and R. J. Madix, *J. Catal.*, **1978**, 53, 208.
[17] J. N. Russell, S. M. Gates and J. T. Yates, *Surf. Sci.*, **1985**, 163, 516.
[18] J. N. Russell, I. Chorkendorff and J. T. Yates, *Surf. Sci.*, **1987**, 183, 316.
[19] L. J. Zielinski and P. N. Sen, *Journal of Magnetic Resonance*, **2003**, 165, 153.
[20] S. W. Rutherford, C. Nguyen, J. E. Coons and D. D. Do, *Langmuir*, **2003**, 19, 8335.
[21] S. Stempel, M. Bäumer and H. J. Freund, *Surf. Sci.*, **1998**, 404, 424.
[22] U. Diebold, J. F. Anderson, K. O. Ng and D. Vanderbilt, *Phys. Rev. Lett.*, **1996**, 77, 1322.
[23] U. Diebold, J. Lehman, T. Mahmoud, M. Kuhn, G. Leonardelli, W. Hebenstreit, M. Schmid and P. Varga, *Surf. Sci.*, **1998**, 411, 135.
[24] C. M. Greenlief, R. I. Hedge and J. M. White, *J. Phys. Chem.*, **1985**, 89, 5681.
[25] T. S. Rufael, D. R. Huntley, D. R. Mullins and J. L. Gland, *J. Phys. Chem.*, **1995**, 99, 11472.
[26] D. R. Huntley, S. L. Jordan and F. A. Grimm, *J. Phys. Chem.*, **1992**, 96, 1409.
[27] K. A. Dickens and P. C. Stair, *Langmuir*, **1998**, 14, 1444.
[28] U. Diebold, *Appl. Phys. A*, **2003**, 76, 681.
[29] M. A. Henderson, W. S. Epling, C. L. Perkins, C. H. F. Peden and U. Diebold, *J. Phys. Chem. B*, **1999**, 103, 5328.
[30] A. Linsebigler, G. Lu and J. T. Yates, *J. Chem. Phys.*, **1995**, 103, 9438.
[31] L. Q. Wang, K. F. Ferris, A. N. Shultz, D. R. Baer and M. H. Engelhard, *Surf. Sci.*, **1997**, 380, 352.
[32] M. A. Henderson, J. Szanyi and C. H. F. Peden, *Catal. Today*, **2003**, 85, 251.
[33] J. A. Rodriguez, T. Jirsak, G. Liu, J. Hrbek, J. Dvorak and A. Maiti, *J. Am. Chem. Soc.*, **2001**, 123, 9597.
[34] M. A. Henderson, *Langmuir*, **1996**, 12, 5093.
[35] E. Farfan-Arribas and R. J. Madix, *Surf. Sci.*, **2003**, 544, 241.
[36] R. E. Tanner, Y. Liang and E. I. Altman, *Surf. Sci.*, **2002**, 506, 251.

[37] X. Guo, J. Yoshinobu and J. T. Yates, *J. Phys. Chem.*, **1990**, 94, 6839.
[38] A. Berkó, T. Bíró and F. Solymosi, *J. Phys. Chem. B*, **2000**, 104, 2506.
[39] D. Ciuparu, F. Bozon-Verduraz and L. Pfefferle, *J. of Phys. Chem. B*, **2002**, 106, 3434.
[40] M. Bowker, R. D. Smith and R. A. Bennett, *Surf. Sci.*, **2001**, 478, L309.
[41] R. A. Bennet, P. Stone, R. D. Smith and M. Bowker, *Surf. Sci.*, **2000**, 454-456, 390.
[42] C. C. Kao, S. C. Tsai, M. K. Bahl, Y. W. Chung and W. J. Lo, *Surf. Sci.*, **1980**, 95, 1.
[43] H. Onishi, T. Aruga, C. Egawa and Y. Iwasawa, *Surf. Sci.*, **1990**, 233, 261.
[44] P. L. Cao, D. E. Ellis and V. P. Dravid, *J. Mater. Res.*, **1999**, 14, 3684.
[45] C. R. Henry, *Surf. Sci. Rep.*, **1998**, 31, 231.
[46] C. C. Chusuei, X. Lai, K. Luo and D. W. Goodman, *Top. Catal.*, **2001**, 14, 71.
[47] M. C. J. Bradford and M. A. Vannice, *Appl. Catal. A*, **1996**, 142, 73.
[48] S. J. Tauster, *Acc. Chem. Res.*, **1987**, 20, 389.
[49] J. S. Smith, P. A. Thrower and M. A. Vannice, *J. Catal.*, **1981**, 68, 270.
[50] S. Takatani and Y. W. Chung, *Appl. Surf. Sci.*, **1984**, 19, 341.
[51] G. B. Raupp and J. A. Dumesic, *J. Catal.*, **1986**, 97, 85.
[52] T. Osaki, *J. Chem. Soc. Faraday T.*, **1997**, 93, 643.
[53] J. vandeLoosdrecht, A. M. vanderKraan, A. J. vanDillen and J. W. Geus, *J. Catal.*, **1997**, 170, 217.
[54] R. Burch and A. R. Flambard, *J. of Catal.*, **1982**, 78, 389.
[55] G. B. Raupp and J. A. Dumesic, *J. of Phys. Chem.*, **1984**, 88, 660.
[56] J. A. Dumesic, S. A. Stevenson, R. D. Sherwood and R. T. K. Baker, *J. Catal.*, **1986**, 99, 79.
[57] O. Dulub, W. Hebenstreit and U. Diebold, *Phys. Rev. Lett.*, **2000**, 84, 3646.
[58] D. R. Jennison, O. Dulub, W. Hebenstreit and U. Diebold, *Surf. Sci.*, **2001**, 492, L677.
[59] F. Pesty, H.-P. Steinrück and T. E. Madey, *Surf. Sci.*, **1995**, 339, 83.
[60] A. Berko, J. Szoko and F. Solymosi, *Surf. Sci.*, **2003**, 532, 390.
[61] J. Szoko and A. Berko, *Vacuum*, **2003**, 71, 193.
[62] A. Berkó, I. Ulrych and K. C. Prince, *J. Phys. Chem. B*, **1998**, 102, 3379.
[63] A. Berkó and F. Solymosi, *Surf. Sci.*, **1998**, 400, 281.
[64] A. Berkó, G. Mensesi and F. Solymosi, *Surf. Sci.*, **1997**, 372, 202.
[65] R. A. Bennett, P. Stone and M. Bowker, *Faraday Discuss.*, **2000**, 114, 267.
[66] T. Suzuki and R. Souda, *Surf. Sci.*, **2000**, 448, 33.
[67] U. Diebold, J. M. Pan and T. E. Madey, *Surf. Sci.*, **1995**, 333, 845.
[68] C. T. Campbell, *Surf. Sci. Rep.*, **1997**, 27, 1.
[69] M. Aizawa, S. Lee and S. L. Anderson, *J. of Chem. Phys.*, **2002**, 117, 5001.
[70] I. V. Yudanov, R. Sahnoun, K. M. Neyman, N. Rosch, J. Hoffmann, S. Schauermann, V. Johanek, H. Unterhalt, G. Rupprechter, J. Libuda and H. J. Freund, *J. Phys. Chem. B*, **2003**, 107, 255.
[71] D. A. H. Cunningham, W. Vogel, R. M. T. Sanchez, K. Tanaka and M. Haruta, *J. Catal.*, **1999**, 183, 24.
[72] G. Rupprechter, H. Unterhalt, M. Morkel, P. Galletto, L. J. Hu and H. J. Freund, *Surf. Sci.*, **2002**, 502, 109.
[73] S. Schauermann, J. Hoffmann, V. Johanek, J. Hartmann, J. Libuda and H. J. Freund, *Catal. Lett.*, **2002**, 84, 209.
[74] J. A. Stroscio and D. T. Pierce, *Phys. Rev. B*, **1994**, 49, 8522.
[75] R. E. Tanner, I. Goldfarb, M. R. Castell and G. A. D. Briggs, *Surf. Sci.*, **2001**, 486, 167.

[76] Z. Xu, L. Surnev, K. J. Uram and J. T. Yates, *Surf. Sci.*, **1993**, 292, 235.
[77] J. B. Miller, H. R. Siddiqui, S. M. Gates, J. N. Russell, J. T. Yates, J. C. Tully and M. J. Cardillo, *Journal of Chemical Physics*, **1987**, 87, 6725.
[78] M. Trenary, K. J. Uram and J. T. Yates, *Surf. Sci.*, **1985**, 157, 512.
[79] C. S. Feigerle, S. H. Overbury and D. R. Huntley, *J. Chem. Phys.*, **1991**, 94, 6264.
[80] A. J. Muscat and R. J. Madix, *J. Phys. Chem.*, **1996**, 1000, 9807.
[81] N. Vasquez, A. Muscat and R. J. Madix, *Surf. Sci.*, **1994**, 301, 83.
[82] J. L. Gland, R. J. Madix, R. W. McCabe and C. Demaggio, *Surf. Sci.*, **1984**, 143, 46.
[83] S. Johnson and R. J. Madix, *Surf. Sci.*, **1981**, 108, 77.
[84] J. C. Bertolini and B. Tardy, *Surf. Sci.*, **1981**, 1981, 131.
[85] J. C. Bertolini, G. Dalmai-Imelik and J. Rousseau, *Surf. Sci.*, **1977**, 68, 539.

REPORT DOCUMENTATION PAGE (SF298)
(Continuation Sheet)

a. Papers published in peer-reviewed journals

1. S. Ma, J. Zhou, Y. C. Kang, J. E. Reddic and D. A. Chen, "Dimethyl Methylphosphonate Decomposition on Cu Surfaces: Supported Cu Nanoclusters and Films on TiO_2(110)," *Langmuir,* **2004**, 20 (2), 9686-9694.

2. K. Varazo, F. W. Parsons, S. Ma and D. A. Chen, "Methanol Chemistry on Cu and Oxygen-covered Cu Nanoclusters Supported on TiO_2(110)," *J. Phys. Chem. B*, **2004**, 108(47), 18274-18283.

3. Illingworth, J. Zhou, O. Osturk, and D. A. Chen, "Design of a Heating-Cooling Stage for STM and TPD Experiments," *J. Vac. Sci. Technol. B,* **2004**, 22(5), 2552-2554.

4. J. Zhou, S. Ma, Y. C. Kang and D. A. Chen, "Dimethyl Methylphosphonate Decomposition on Titania-Supported Ni Clusters and Films: A Comparison of Chemical Activity on Different Ni Surfaces," *J. Phys. Chem. B* , **2004**, 108, 11633-11644.

5. J. Zhou, Y. C. Kang and D. A. Chen, "Adsorbate-induced Dissociation of Metal Clusters: TiO_2(110)-supported Cu and Ni Clusters Exposed to Oxygen Gas, " *Surf. Sci.*, **2004**, 562(1-2), 113-127.

6. J. Zhou, K. Varazo, J. E. Reddic, M. L. Myrick and D. A. Chen, "Decomposition of Dimethyl Methylphosphonate on TiO_2(110): Principal Component Analysis Applied to X-Ray Photoelectron Spectroscopy," *Analytica Chimica Acta,* **2003**, 496, 289-300.

7. J. Zhou, Y. C. Kang, and D. A. Chen, "Oxygen-induced Dissociation of Cu Islands on TiO_2(110)," *J. Phys. Chem B.,* **2003**, 107(28), 6664-6667.

8. J. Zhou, Y. C. Kang and D. A. Chen, "Controlling Island Size Distributions: A Comparison of Nickel and Copper Growth on TiO_2(110)," *Surf. Sci.* **2003**, 537, L429-L434.

9. J. Zhou and D. A. Chen, "Controlling Size Distributions of Copper Islands Grown on TiO_2(110)-(1x2)," *Surf. Sci.*, **2003**, 527, 183-187.

10. J. E. Reddic, J. Zhou, and D. A. Chen, "Scanning Tunneling Microscopy Studies of the Growth of Cu Clusters on a Reconstructed TiO_2(110)-(1x2) Surface," *Surf. Sci.*, **2001**, 494, L767.

b. Papers published in non peer-reviewed journals or conference proceedings

None

c. Papers presented at meetings but not in conference proceedings

1. "Exploring the Growth of Copper Clusters on TiO_2(110)," J. E. Reddic, J. Zhou, B. T. Long and D. A. Chen, Regional American Vacuum Society Meeting, Orlando FL, March 12-15, 2001.
2. "New Catalysts for the Decomposition of Chemical Warfare Agents: Reactivity of Dimethyl Methyl Phosphonate on Supported Copper Particles on TiO_2(110)-(1x2)," D. A. Chen, J. E. Reddic and J. Zhou; Sorbents and Filtration Workshop, Nashville, TN, April 2001 (invited).
3. "Surface Chemistry on Supported Cu Nanoparticles: Dimethyl Methyl Phosphonate Reaction on Cu/TiO_2(110)-(1x2)," D. A. Chen, J. Zhou and J. E. Reddic; American Vacuum Society, San Francisco, CA, October-November 2001.
4. "Scanning Tunneling Microscopy Studies of the Growth and Morphology of Cu Clusters Deposited on TiO_2(110)," J. Zhou, J. E. Reddic, and D. A. Chen; American Vacuum Society, San Francisco, CA, October-November 2001 (poster).
5. "Dimethyl Methylphosphonate Reaction on Cu Particles Deposited on a TiO_2(110)-(1x2) surface" J. Zhou, K. Varazo, J. E. Reddic, and D. A. Chen; American Chemical Society, Orlando, FL 2002.
6. "Metal Island Growth on Oxide Surfaces: STM Studies of Copper Islands on TiO_2(110)" J. Zhou, J. E. Reddic, K. Varazo, and D. A. Chen; American Chemical Society, Orlando, FL April 2002.
7. "Controlling Island Size Distributions for Metals on Oxides: Copper and Nickel Islands on TiO_2(110)-(1x2)," J. Zhou, J. E. Reddic, and D. A. Chen; American Vacuum Society, Denver, CO November 2002.
8. "Dimethyl Methylphosphonate Reaction on Metal Nanoparticles Deposited on a TiO_2(110)-(1x2) Surface," J. Zhou, K. Varazo and D. A. Chen; American Vacuum Society, Denver, CO, November 2002.
9. "Decomposition of Dimethyl Methylphosphonate on Metal Nanoparticles Deposited on a TiO_2(110) Surface," J. Zhou, S. Ma, Y. C. Kang and D. A. Chen; American Chemical Society, Division of Colloid and Surface Science, Atlanta, GA June 2003.
10. "Dimethyl Methylphosphonate Decomposition on Supported Ni nanoparticles Deposited on a TiO_2(110) Surface" J. Zhou, S. Ma, Y. C. Kang, and D. A. Chen; American Vacuum Society, Baltimore, MD November 2003.
11. "Oxygen-induced Morphological Changes in Cu and Ni Islands on TiO_2(110)," J. Zhou, S. Ma, Y. C. Kang and D. A. Chen; American Vacuum Society, Baltimore, MD November 2003.
12. "Scanning Tunneling Microscopy Studies of Cu Growth on TiO_2(110)," J. Zhou, Y. C. Kang and D. A. Chen; South Carolina Academy of Sciences, Clemson, SC April 2003.

13. "Decomposition of Dimethyl Methylphosphonate on TiO2-Supported Copper and Nickel Nanoclusters," J. Zhou, S. Ma, Y. C. Kang and D. A. Chen, Center for Functional Nanomaterials Users Meeting, Upton, NY (Brookhaven National Laboratory) May 20, 2004 (invited).

14. "Decomposition of Dimethyl Methylphosphonate on TiO_2-Supported Ni Nanoclusters", J. Zhou, S. Ma, Y. C. Kang and D. A. Chen, American Vacuum Society Meeting, Anaheim, CA, November 19, 2004.

d. Manuscripts submitted but not published
None

e. Technical reports submitted to ARO
Interim report 9/00-3/01
Interim report 3/01-9/01
Interim report 9/01-9/02
Interium report 9/02-9/03

Scientific personnel
Jing Zhou, graduate student (9/00-5/04), Ph.D. May 2004
John Reddic, postdoctoral associate (9/00-8/01)

Report of inventions
None